UTAH GEOLOGICAL SURVEY
a division of
Utah Department of Natural Resources

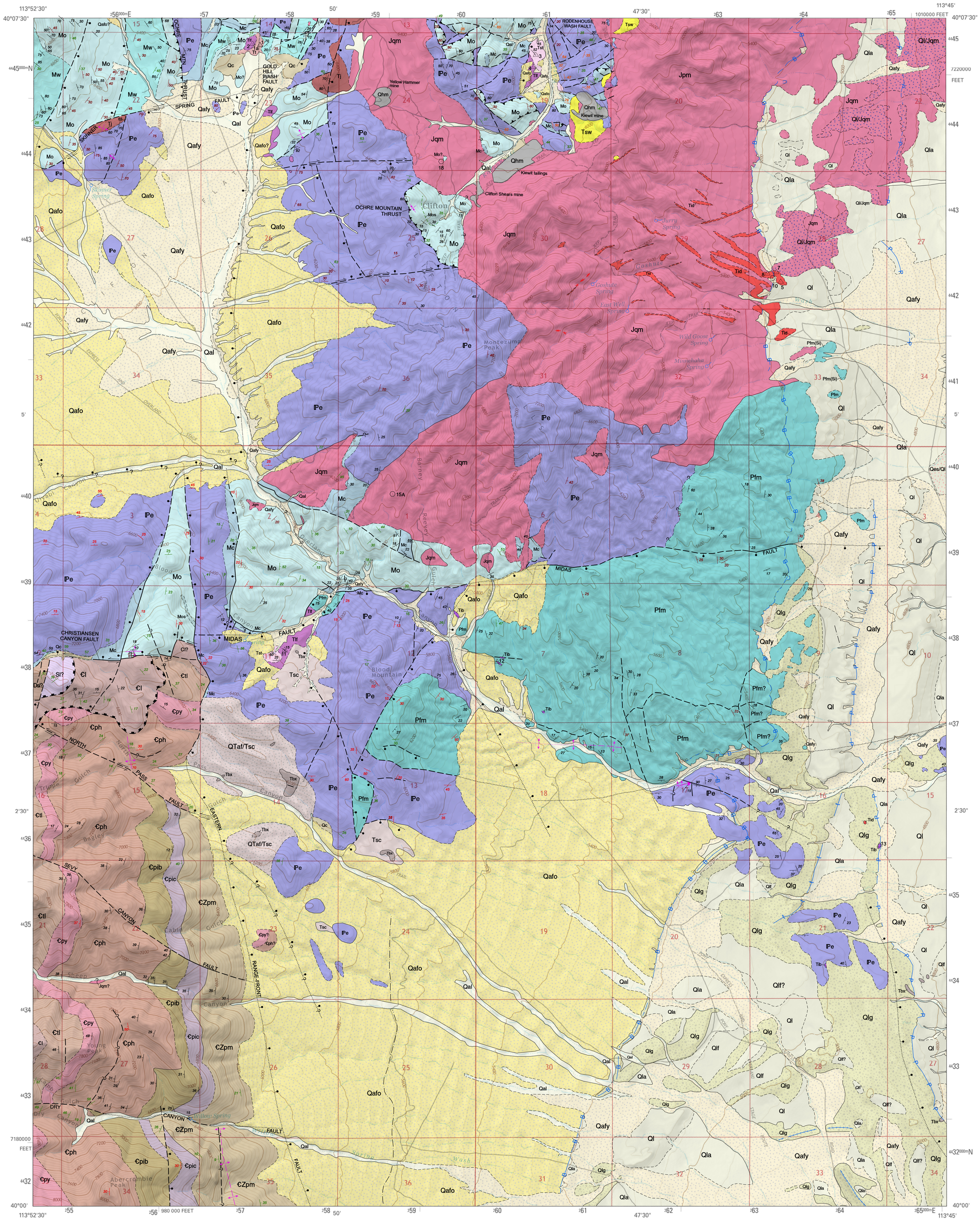

This open-file release makes information available to the public that has undergone only minimal peer review and may not conform to Utah Geological Survey technical, editorial, or policy standards. The map may be incomplete, and inconsistencies, errors, and omissions have not been resolved. The Utah Department of Natural Resources, Utah Geological Survey, makes no warranty, expressed or implied, regarding the suitability of this product for a particular use, and does not guarantee accuracy or completeness of the data. The Utah Department of Natural Resources, Utah Geological Survey, shall not be liable under any circumstances for any direct, indirect, special, incidental, or consequential damages with respect to claims by users of this product. For use at 1:24,000 scale.

This geologic map was funded by the U.S. Geological Survey through Earth MRI award number G20AC00168 (2020-22).

This map was created from geographic information system (GIS) files. The UGS does not guarantee accuracy or completeness of the data. Persons or agencies using these data specifically agree not to misrepresent the data, nor to imply that changes they made were approved by the Utah Geological Survey and should indicate the data source and any modifications they make on plots, digital copies, derivative products, and in metadata.

11°32'
TRUE NORTH
MAGNETIC NORTH
APPROXIMATE MEAN DECLINATION, 2023

SCALE 1:24,000

1 0.5 0 1 MILE

1000 0 1000 2000 3000 4000 5000 6000 7000 FEET

1 0.5 0 1 KILOMETER

CONTOUR INTERVAL 40 FEET

UTAH
MAP LOCATION

Base modified from USGS US Topo Clifton 7.5' Quadrangle (2011, 2014, and 2020)
Shaded relief derived from USGS 10-meter NED
Projection: UTM Zone 12
Datum: NAD 1983

Program Manager: Stefan M. Kirby
GIS and Cartography: Rosemary Fasselin, Subigya Shah, Donald L. Clark, Andrew Rupke, and Stephanie E. Mills
GIS review: Josh A. Dustin and Austin J. Jensen

Utah Geological Survey
1594 West North Temple, Suite 3110
Salt Lake City, UT 84116
(801) 537-3300
https://geology.utah.gov
https://doi.org/10.34191/OFR-752DM

1	2	3
4	·	5
6	7	8

1. Ochre Mountain
2. Gold Hill
3. Gold Hill Wash
4. Ibapah
5. Goshute Wash
6. Goshute
7. Goshute Canyon
8. Callao

ADJOINING 7.5' QUADRANGLE NAMES

INTERIM GEOLOGIC MAP OF THE CLIFTON QUADRANGLE, TOOELE COUNTY, UTAH

by

Stephanie E. Mills, Andrew Rupke, and Donald L. Clark

2023

CORRELATION OF GEOLOGIC UNITS

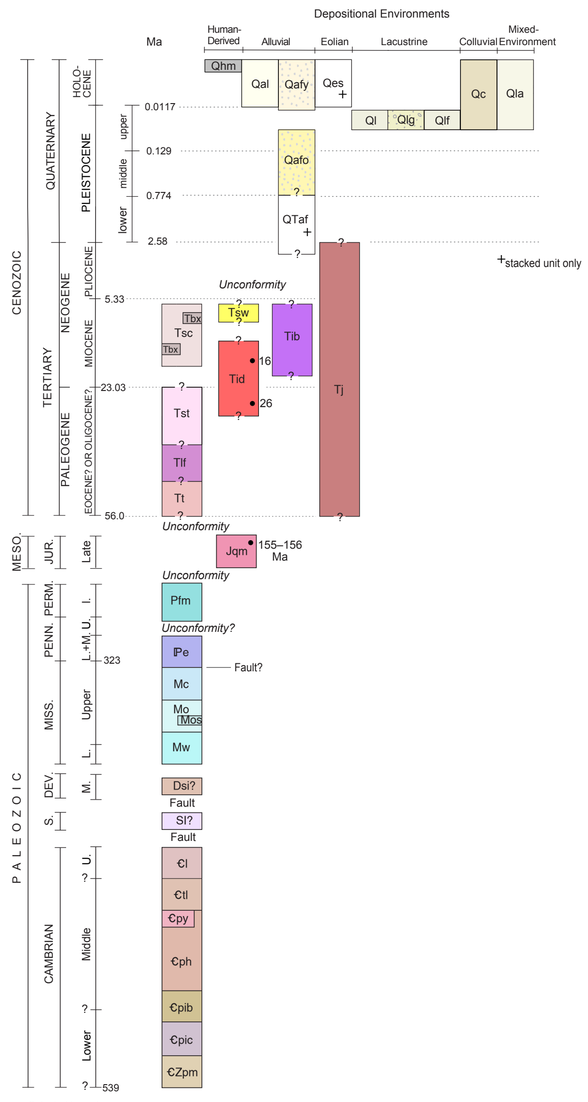

Selected boundary ages from International Chronostratigraphic chart v2023/04.

GEOLOGIC SYMBOLS

- Contact – dashed where approximately located, dashed and queried where existence and location uncertain
- Marker bed – dashed where approximately located (unit Mos)
- High-angle normal fault – dashed where approximately located, dashed and queried where approximately located and existence uncertain, dotted and queried where existence and location uncertain; bar and ball on downthrown side
- Low-angle normal fault - dashed where approximately located; teeth on hanging wall
- Oblique-slip fault - dashed where approximately located, dotted where concealed, dotted and queried where existence and location uncertain; arrows/bar and ball indicate relative displacement
- Thrust fault - dashed where approximately located, dotted where concealed; teeth on hanging wall
- Fault of unknown geometry and kinematics - dashed where approximately located, dashed and queried where approximately located and existence uncertain, dotted where concealed, dotted and queried where existence and location uncertain
- Lineament – from aerial imagery interpretation
- Igneous dike (unit Tid)
- Axial trace of anticline - dashed where approximately located, dotted where concealed; symbols: straight arrows for upright, curved arrows for overturned, large arrow for plunge
- Minor anticline
- Minor syncline
- Lake Bonneville shorelines (elevation data in Currey, 1982; Chen and Maloof, 2017) – dashed where approximately located
  - B – Bonneville shoreline 5240-5200 feet (1598-1585 m)
  - t – Transgressional shoreline 5040-4980 feet (1537-1518 m)
  - P – Provo shoreline zone 4880-4840 feet (1488-1476 m)
- Beach ridge crest
- Sedimentary bedding attitude – field measured in black; data from other sources in red (Nolan, 1935, plate 1), dark red (Nolan, 1935, plate 2), green (Malan, 1989), and orange (Robinson, 2006 unpublished, 2016)
  - 20 – Inclined
  - 30 – Inclined, approximate
  - Vertical
- Foliation or layering in volcanic rock
- 10 – Geochronology sample and ID
- 5 – Geochemistry sample and ID
- Spring

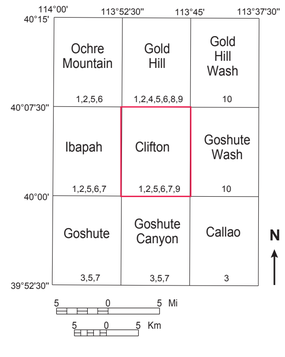

1. Nolan, 1935 (plate 1, 1:62,500)
2. Nolan, 1935 (plate 2, 1:24,000)
3. Bick, 1966 (1:66,172)
4. El-Shatoury, 1967 (1:600)
5. Thomson, 1973 (plate 2, 1:63,360 compilation; plates 3 and 5)
6. Malan, 1989 (1:24,000)
7. Rodgers, 1989 (1:50,000)
8. Robinson, 1993 (1:24,000)
9. Robinson, 2006 unpublished, 2016
10. Clark and others, 2016 (1:75,000)

Index to geologic mapping near the Clifton 7.5' quadrangle

GEOLOGIC UNITS

Qhm	Mining disturbances
Qal	Stream alluvium
Qafy	Younger fan alluvium
Qafo	Older fan alluvium
Ql	Lacustrine deposits, undivided
Qlg	Lacustrine gravel
Qlf	Lacustrine fine-grained deposits
Qc	Colluvium
Qla	Lacustrine and alluvial deposits, undivided
Qes/Ql	Eolian sand over undivided lacustrine deposits
Ql/Jqm	Undivided lacustrine deposits over Jurassic quartz monzonite
QTaf/Tsc	High-level fan alluvium over Salt Lake Formation conglomerate
Tj	Jasperoid
Tsw	Quartz stockwork
Tsc	Salt Lake Formation, conglomerate
Tbx	Dolomite breccia
Tid	Igneous dikes, undivided
Tib	Basalt dikes
Tst	Volcaniclastic sandstone and tuff
Tlf	Lava flows
Tt	Welded tuff
Jqm	Jurassic quartz monzonite
Pfm Pfm?	Ferguson Mountain Formation [locally silicified, Si]
IPe IPe?	Ely Limestone
Mc	Chainman Formation
Mo Mo?	Ochre Mountain Limestone
Mos	Ochre Mountain Limestone, shale member
Mw	Woodman Formation
Dsi?	Simonson Dolomite?
Sl?	Laketown Dolomite?
Ꞓl Ꞓl?	Lamb Dolomite
Ꞓtl	Trippe Limestone
Ꞓpy Ꞓpy?	"Pierson Cove" Formation, Young Peak dolomite member
Ꞓph Ꞓph?	"Pierson Cove" through Howell Formations, undivided
Ꞓpib	Pioche Formation, Busby Quartzite Member
Ꞓpic	Pioche Formation, Cabin Shale Member
ꞒZpm	Prospect Mountain Quartzite

LITHOLOGIC COLUMN

CHRONO-STRATIGRAPHIC UNIT			GEOLOGIC UNIT		MAP SYMBOL	THICKNESS Feet (Meters)	LITHOLOGY / NOTES
Overlain by Q-T surficial deposits							
T.	NEO.	Mio.	Salt Lake Fm	dol bx	Tsc Tbx	100+ (30+)	also Tid and Tib dikes
T.	PAL.	Olig-Eo?	volcanic rocks	see notes		~250 (75)	Tid, Tst,Tlf, Tt
UNCONFORMITY							Jqm 155–156 Ma quartz monzonite pluton
PERMIAN		lower	Ferguson Mountain Formation		Pfm	1745+ (530+)	Commonly less resistant and deformed
UNCONFORMITY?							
PENNSYLVANIAN		Lower - Middle	Ely Limestone		IPe	2160–3520+ (660–1075+)	Cyclic lithologies
M.		U.	Chainman Formation		Mc	450± (140±)	Weak, highly deformed unit
FAULT?							
MISSISSIPPIAN		Upper	Ochre Mtn Limestone	Sh. mbr	Mo Mos	<1050 (<320) 0–50 (0–15)	
MISSISSIPPIAN		Upper–Lower	Woodman Formation		Mw	<1500 (<460)	
D.		M.	Sim. Dol?		Dsi?	~200 (60)	
FAULT							
SIL.			Laketown Dolomite?		Sl?	570 (145)	
FAULT							
CAMBRIAN		U.	Lamb Dolomite		Ꞓl	460+ (140+)	
CAMBRIAN		Middle	Trippe Limestone		Ꞓtl	660–765 (180–235)	•=Trilobites
CAMBRIAN		Middle	Young Peak dol Mbr		Ꞓpy	0–600 (0–180)	
CAMBRIAN		Middle	"Pierson Cove" through Howell Formations		Ꞓph	2500–2700 (760–825)	"Pierson Cove" Fm; Wheeler Sh; Swasey Ls; Whirlwind Fm; Dome Ls; Chisholm Sh; Howell Fm
CAMBRIAN		Lower	Pioche Fm	Busby Qtz Mbr	Ꞓpib	410–450 (125–135)	
CAMBRIAN		Lower	Pioche Fm	Cabin Shale Mbr	Ꞓpic	500 (150)	
CAMBRIAN		Lower	Prospect Mountain Quartzite		ꞒZpm	800+ (245+)	Resistant Cliffs; lower part not exposed

INTERIM GEOLOGIC MAP OF THE CLIFTON QUADRANGLE, TOOELE COUNTY, UTAH

by

Stephanie E. Mills, Andrew Rupke, and Donald L. Clark

Suggested citation:

Mills, S.E., Rupke, A., and Clark, D.L., 2023, Interim geologic map of the Clifton quadrangle, Tooele County, Utah: Utah Geological Survey Open-File Report 752DM, 22 p., 2 plates, scale 1:24,000, https://doi.org/10.34191/OFR-752DM.

Disclaimer

This geologic map was funded by the U.S. Geological Survey through Earth MRI award number G20AC00168 (2020–22).

OPEN-FILE REPORT 752DM
UTAH GEOLOGICAL SURVEY
UTAH DEPARTMENT OF NATURAL RESOURCES
2023

CONTENTS

FIGURES

TABLES

PLATES

INTRODUCTION

The Clifton 7.5' quadrangle is in western Tooele County about 40 miles (65 km) south of Wendover, Utah. The northeast part of the quadrangle includes the Clifton Hills and the southwest part includes the northern Deep Creek Range/Mountains. These uplands are separated by Overland Canyon and Clifton Flat (figure 1, plate 1). The quadrangle is in the Basin and Range physiographic province between the Great Salt Lake Desert to the east and Deep Creek Valley to the west. Terrain and vegetation are typical of the Basin and Range province and include rugged mountains separated by adjoining basins. Notable geographic landmarks within the mapping area include Montezuma Peak, Clifton Flat, Blood Mountain, Young Peak, and Abercrombie Peak. To the north of the quadrangle a few people reside in the hamlet of Gold Hill, which is named for an old mining outpost; however, no permanent settlement exists within the Clifton quadrangle. The area is accessible via U.S. Highway 93 south from Wendover then east on the Ibapah Road and following maintained paved and gravel roads to the Gold Hill townsite and south, or directly east to the Clifton map area. The area can also be accessed about 115 miles (185 km) northwest of Delta by mostly gravel roads. Land ownership in the quadrangle is primarily public (Federal and State), with private land on patented ground around significant mining areas. The northern part of the quadrangle (Clifton Hills area) contains the southern half of the Gold Hill mining district, periodically active since the late 1800s. The northern end of the Deep Creek Range/Mountains is covered by the Deep Creek Mountains Wilderness Study Area. To the east is the U.S. Army Dugway Proving Ground, whereas to the northeast is the U.S. Air Force Utah Test and Training Range-South area. Active uses of the quadrangle include mining, transportation, agriculture, and recreation.

This geologic map (plates 1 and 2) is part of the U.S. Geological Survey (USGS) Earth Mapping Resources Initiative (Earth MRI) program in partnership with the National Cooperative Geologic Mapping Program (NCGMP). Mapping was conducted as part of a larger project assessing critical mineral potential in the district, with an emphasis on tungsten. The production of a new map of the Clifton quadrangle occurred along with the digital reproduction of prior mapping of the Gold Hill quadrangle to the north (Robinson, 1993). These two quadrangles cover the majority of minerals-related areas within the Gold Hill mining district.

Map data were compiled from several prior sources and new mapping efforts. Only intermediate-scale mapping from Nolan (1935) existed for the entire quadrangle, though detailed mapping of the Gold Hill-Clifton Hills area is in the same publication. More recent mapping from Thomson (1973), Malan (1989), and Rodgers (1989) covers most of the western part of the quadrangle, and Thomson (1973) also included detailed mapping around the Blood Canyon fault. Minerals-industry mapping from unpublished Utah Geological Survey (UGS) files includes detailed mapping around the Kiewit mine area (also see Robinson, 2016). Additional revisions to this quadrangle area may occur in subsequent years as the UGS undertakes intermediate-scale mapping of the area.

Unpublished airborne magnetic and radiometric data from minerals-industry surveys were used to map some concealed faults. The extent of these surveys covered the Gold Hill mining district and extended across the Blood Canyon fault into the very northern end of the Deep Creek Range, as well as extending west into Nevada. The magnetic and radiometric data used were interpreted as a magnetic grid as well as the potassium channel, thorium channel, and uranium channel from aeroradiometrics.

New geochemical samples were collected in a general 1150 foot-spaced (350 m)- grid over mineralized areas along the contact between Paleozoic strata and Jurassic and Eocene igneous intrusions. These samples are part of the associated UGS study on the critical mineral potential of the Gold Hill mining district. Additional targeted lithologic samples of volcanic units and intrusive dikes were collected; sample locations are shown on plate 1 and results are presented in figure 2, and tables 1 and 2.

GEOLOGIC OVERVIEW

The Gold Hill district and northern Deep Creek Range area is characterized by Neoproterozoic metasedimentary rocks overlain by passive margin Paleozoic strata. This stratigraphy was intruded and deformed by temporally overlapping magmatic and tectonic events. The quadrangle is near a long-lived east-west-trending structural zone known as the Cortez-Uinta axis among other names (Roberts and others, 1965; Clark, 2020). The area is also part of the hinterland of the Jurassic to Paleogene North American Cordilleran orogenic system (Armstrong, 1968; Yonkee and Weil, 2015). The hinterland represents a zone between the Luning Fencemaker fold-thrust belt of Nevada and the Sevier fold-thrust belt in Utah. This zone is locally characterized by: 1) intrusion of Middle-Late Jurassic plutons and limited shortening, 2) Cretaceous and Paleogene crustal thickening and metamorphic core complex development, 3) Eocene to Miocene volcanism, and 4) subsequent extension and modern basin formation.

The Jurassic plutons are interpreted to have been emplaced along pre-existing faults and are possibly related to a minor period of extension during the Early Jurassic, though timing and mechanism of this event is poorly constrained (Wernicke and Burchfiel, 1982; Miller, 1990; Robinson, 1993; Miller and Hoisch, 1995; Yonkee and Weil, 2015). From the Late Cretaceous to Paleogene the over-thickened crust of the hinterland formed a broad orogenic plateau (DeCelles, 2004). The major tectonic regime shift (slab removal) during the Eocene to Oligocene drove an episode of spatially limited extension and magmatism (Best and Christiansen, 1991; Yonkee and Weil, 2015). Basin and Range extensional tectonics, and bimodal volcanism began about 20 Ma (Miocene) and continues to the present (see Christiansen and McKee, 1978; Zoback, 1983). The basins in northwest Utah preserve a thick package of sedimentary and volcanic rocks (~17 to 6 Ma) deposited during early basin and range extension.

The geology in the Gold Hill district-northern Deep Creek Range area includes extensively faulted Cambrian to Permian siliciclastic and carbonate rocks intruded by an aerially extensive Jurassic pluton, a smaller Eocene stock, and Tertiary dikes. The sequence is overlain by Tertiary extrusive volcanic rocks and Miocene sedimentary rocks mantled by Quaternary-Tertiary surficial deposits. Mineralization is associated with the intrusive rocks and is discussed further below.

The Jurassic pluton, which intrudes Mississippian, Pennsylvanian, and Permian strata, is exposed over 19 mi^2 (50 km^2), and has been described as either quartz monzonite (Nolan, 1935; Burwell, 2018) or granodiorite (Robinson, 1993). Geochemistry from the associated UGS minerals report (in progress) indicates a quartz monzonite composition (figure 2, table 1). The Jurassic intrusion has been dated to 155–156 Ma by U-Pb zircon (Burwell, 2018) updating prior K-Ar ages (Stacey and Zartman, 1978) (figure 3, table 2). The Eocene stock is compositionally a granite to granodiorite (figure 2, table 1) and has a 40 Ma U-Pb zircon age (King and Burwell, 2016) that updates prior K-Ar ages (Stacey and Zartman, 1978) (figure 3, table 2). Other minor intrusive units in the district include: 1) a small diorite intrusion north of the Eocene stock with a 40 Ma U-Pb zircon age (King and Burwell, 2016), 2) a granite dike cutting the north end of the Jurassic quartz monzonite with a 40 Ma U-Pb zircon age (Burwell, 2018), 3) a monzonite dike cutting the northeastern corner of the Jurassic quartz monzonite with an age of 17 Ma (U-Pb zircon, Burwell, 2018), and 4) a granite dike in the Goshute Wash area with an age of 16 Ma (U-Pb zircon, this study) (figure 2, table 2). There are a multitude of other minor intrusive phases reported to be in the district, including aplite, andesite, and latite dikes, but they have no age control (Robinson, 1993; Burwell, 2018).

The Goshute Wash area contains a dense dike swarm with three recognized compositions ranging from granitic to basaltic, with the granitic dike providing the only age control. This dike previously yielded a K-Ar on feldspar concentrate age of 27 Ma (unpublished data [1974] from AMAX exploration company reported by Krahulec [2017]), which is notably older than the 16 Ma age obtained in this study (figure 3, table 2). We interpret our Miocene U-Pb age to be the more reliable of the two. The interrelated style of emplacement for all compositions suggests compositions are broadly coeval. Interpretation by AMAX geologists suggested the felsic dikes are the youngest composition. All compositions of the Goshute Wash dike swarm are cut by northeast-trending, blocky quartz-carbonate veins interpreted as a late Miocene feature (possibly related to late Miocene mineralization in Rodenhouse Wash) (e.g., El-Shatoury and Whelan, 1970). These veins show internal brecciation and multiple generations of growth, indicating they were emplaced during deformation. Therefore, more geochronology on the Goshute Wash dike swarm and vein network is needed. In addition, other undated basaltic dikes are present near Overland Canyon and south of Goshute Wash.

A number of undated Tertiary volcanic rock units are mapped across the northern and central map area. Compositions of the volcanics vary from intermediate to rhyolitic (figure 2A) and though most appear to be extrusive lava flows and welded tuff, a rhyolitic volcaniclastic unit in the Rodenhouse Wash and Blood Canyon area is clearly water-lain with well-developed cross-bedding (table 1). Miocene basin-fill rocks are mainly mapped in the western valley margin area near Blood Mountain. Altered areas include jasperoid and quartz vein stockwork largely at the Kiewit mine area.

Bedrock units are overlain by latest Tertiary and Quaternary surficial deposits primarily related to alluvial and lacustrine environments. Stream alluvium and three levels of alluvial-fan deposits are present. Lake Bonneville impinged on the eastern part of the quadrangle evidenced by the Bonneville and Provo shorelines and associated deposits. Smaller areas of eolian, colluvial, mixed deposits, and mining disturbances also occur.

STRUCTURE IN THE CLIFTON QUADRANGLE

This map presents new and updated structural interpretations that record the complex deformational history in the Gold Hill district and the northern Deep Creek Mountains. Prior geoscientists noted the area is broken into discrete structural blocks (see for example, Burwell, 2018, figure 3). Robinson (1993, 2006) interpreted 15 deformational events throughout the evolution of the district that include Mesozoic folding, thrust faulting and extensional faulting; late Mesozoic-early Tertiary strike-slip and

low-angle normal faulting; and Tertiary low- and high-angle normal faulting. There is a complicated overprinting of compressional and extensional deformation. Two primary igneous intrusions (Jurassic and Eocene in age) and others overprint preexisting structures. Weaker rock units (i.e., Chainman and Woodman Formations) typically accommodated more deformation compared to more resistant units. This interpretation is based on field observations across the map area. However, as noted by Robinson (1990), there are relatively few kinematic indicators such as slickensides or fault fabric to elucidate strain histories. Kinematic symbolization of most faults on plate 1 is inferred based on stratigraphic relationships. However, these depictions are unlikely to represent the entire kinematic history of faults in an area where multiple tectonic events, stratigraphic tilting, rotation, and fault reactivation are likely to have been common.

In the northern part of the map area (southern Gold Hill district), compressional deformation is related to east-directed shortening on the Ochre Mountain thrust fault. In the quadrangle, the Ochre Mountain thrust places Mississippian Chainman, Ochre Mountain, and Woodman Formation rocks on the Pennsylvanian Ely Limestone. Intense deformation near the Jurassic quartz monzonite contact may be associated with thrusting and/or associated pluton emplacement. Much of the compressional deformation observed in outcrop is not resolvable on the scale of the map and includes small-scale thrust faults and folding.

North and east of Clifton Flat we interpret the complex fault network as largely compressional faults with later normal reactivation. We attribute them as unknown and/or oblique-slip faults. The Gold Hill Wash fault is primarily in the Gold Hill quadrangle to the north, but trends to the south until it reaches the Clifton Flat basin in the map area. This fault is interpreted by Robinson (1993) as a north-south dextral strike-slip fault active as late as 10 Ma. However, the stratigraphic relationships along this fault are complex and could be the result of multiple phases of deformation, therefore we map it as a fault with unknown kinematics. The Skinner Spring fault (named here) is an example of an east-west fault with apparent strike-separation and is mapped as an oblique-slip structure that in part bounds northern Clifton Flat.

Extensional deformation in the northern area is associated with normal faulting and brittle to ductile shearing within carbonate units. However, the large-scale low-angle extensional faulting of the Gold Hill area (see Robinson, 1993) is not present here. We interpret Clifton Flat to be a graben bounded by normal faults.

The Paleozoic and Cenozoic rocks at Rodenhouse Wash are surrounded by a Jurassic pluton and represent a roof pendant based on the interpretation of Robinson (unpublished data; 2016). We followed this mapping but note that the Paleozoic units here are altered making unit calls uncertain, the complexity of the map pattern, and map-cross section consistency issues. We did not include his proposed domain boundary and eastern high-angle faults.

The quadrangle is bisected by a major east-west-trending structure called the Blood Canyon fault, originally mapped and named by Nolan (1935). Nolan (1935) reported that this was a transverse fault (left-lateral strike-slip) separating structural blocks. Malan (1989) later interpreted the Blood Canyon fault as a lateral ramp of the Reilly Canyon fault, a low-angle fault mapped by Rodgers (1987, 1989) along the eastern range front of the Deep Creek Range. Miller and others (1999) call this low-angle fault, the Deep Creek Range fault. This fault is offset by another higher-angle normal fault (their figure 4) as shown by Malan (1989). The extent and possible connection of the Reilly Canyon/Deep Creek Range fault northward to the northern Deep Creek Range and map area is uncertain. Mapping for this study indicates that the Blood Canyon fault is two different faults, which we name the Christiansen Canyon fault (west) and Midas fault (east). These two faults are separated by the eastern range-front normal fault (plate 1). Displacements on the Christiansen Canyon and Midas faults are constrained by geologic map patterns and limited smaller-scale secondary structures. The Midas fault bounds the southern margin of the Jurassic pluton and is interpreted as a normal fault with potentially some left-oblique-slip. The Christiansen Canyon fault appears to have a complicated history that we attribute as oblique-slip. It and other nearby faults (Midas, North Pass, Sevy, and Dry Canyon faults, and unnamed low-angle normal faults) help record the complex, multi-phase compressional, extensional and rotational deformation of the map area.

The eastern range-front fault is a north-south-trending, high-angle normal fault of substantial displacement that probably links to the Midas fault. The fault dies out northward near Clifton Flat and the southwest margin of the Jurassic pluton. The range-front fault's hanging wall contains Ely Limestone, Ferguson Mountain Formation, Tertiary volcanic rocks, and Miocene Salt Lake Formation. This fault is on trend with Quaternary normal faults along the eastern range front of the central and southern Deep Creek Mountains (UGS, 2023).

Another significant east-west-trending fault is present south of the Midas fault. This fault is cryptic, but appears to be the southern margin of a graben containing structurally deformed Ferguson Mountain Formation. Ely Limestone south of this fault is also deformed. A concealed normal fault is present near the southeastern map corner as indicated by blocks of poorly exposed Salt Lake Formation dolomite breccia in the hanging wall with Ely Limestone in the foot wall.

ORE DEPOSITS AND MINERAL ENDOWMENT

The timing of emplacement and type of mineral deposits present at Gold Hill are discussed by many authors (Nolan, 1935; Chorney, 1943; El Shatoury and Whelan, 1970; Robinson, 2006; Krahulec, 2017; Carey, 2022). The Gold Hill mining district is one of the oldest in Utah and was mainly active during WWI and WWII, with only sporadic production since. The district is Utah's largest tungsten and arsenic producer, but also produced modest gold, copper, lead, and bismuth. Mineralization can broadly be described as magmatic-hydrothermal in character and timing is controlled by the major magmatic events in the district. Some confusion over the number and age of mineralizing events comes from the lack of detailed geochronology on Tertiary dikes as described above, but is also influenced by overprinting mineralization at individual deposits (e.g., Reaper mine; Carey, 2022). Mineralization associated with the Jurassic and Eocene intrusions is generally agreed upon with respect to timing and has had more study.

Deposits associated with the Jurassic quartz monzonite pluton include skarn, replacement, and polymetallic vein deposits. The only exception to this classification is a set of deposits that have been variably referred to as pegmatite veins (Butler and others, 1920), pipe-like deposits (Nolan, 1935), replacements (El-Shatoury and Whelan, 1970), and pegmatite pipes (Krahulec, 2017). These deposits include the Yellow Hammer, Rustler, Reaper, and Centennial mines. The Reaper mine is considered a type example for this type of mineralization. The classification of these deposits is complicated by: 1) extreme mineral size, for example actinolite from Yellow Hammer has been reported to occur on the foot-scale (Erich Petersen, personal communication to S.E. Mills); 2) mineralogy, most of these deposits have an abundance of tourmaline that has traditionally been interpreted to indicate a pegmatitic influence; and 3) deposit morphology, given that some deposits such as Reaper have a unique vertically elongated shape as opposed to more tabular mantos morphology expected of replacements or intrusion draping morphology typical of skarns. Fieldwork and sampling undertaken as part of this and other UGS studies (Mills, in progress) suggest that these deposits are skarns, as is supported by chemistry in Carey (2022). The large mineral size can be a feature of skarns as the alteration of carbonate units around intrusions tends to be volume-reducing, which allows for growth of large euhedral crystals. The invocation of "pegmatite" classification due to the presence of abundant tourmaline is based on older mineral models where tourmaline is an identifier of pegmatites. Although this can be true, tourmaline can occur in a wide range of non-pegmatitic mineral deposits, including tourmaline breccias associated with porphyry systems (e.g., Frisco district, Beaver County, Utah). There is no evidence for highly fractionated magmatic pegmatites nor for hydrothermal fluids sourced from such magmas, which would have more unique and exotic mineral species than just tourmaline. Likewise, the unique sub-vertical deposit morphology is interpreted to be a result of the complex structural development of the Gold Hill district that likely contributed to irregular pluton boundaries. The availability of favorable bedding horizons influenced fluid flow, mineral zonation, and overall deposit morphology. Hence, the Gold Hill district deposits related to the Jurassic intrusion are classified as skarns, replacements, and polymetallic veins. The skarns are generally copper, gold, and tungsten bearing, whereas the replacement and polymetallic vein deposits also host copper and gold. These deposits are more diverse in mineralogy and range from arsenic-enriched (Gold Hill mine) to molybdenum enriched (Rustler mine) to bismuth and tungsten enriched (Lucy L mine).

Deposits associated with the Eocene granite stock include tungsten skarns and potentially lead-silver replacement and polymetallic vein deposits. Robinson (2006) notes that these deposits have no obvious genetic link to the Eocene stock aside from a spatial relationship. Lead isotopes on feldspars from the Eocene stock and lead ores from several deposits have no apparent correlation, whereas lead isotopes from the Jurassic pluton and lead-bearing minerals in the surrounding deposits show a correlation. An often-cited but less well-defined Eocene deposit type is sediment-hosted gold systems (Carlin Type), which were a major target of exploration for several companies from the 1980s to 2010s. The central Basin and Range is a prolific producer of sediment hosted gold (e.g., the Carlin Trend), and sediment hosted gold is known to occur farther east of Gold Hill in Utah (e.g., Mercur district, Drum mines). Several indicators in Gold Hill have encouraged the idea of a sediment-hosted gold system, such as favorable host rock (typically the Ochre Mountain Limestone), extensive jasperoid development, and low-level stratigraphically restricted gold enrichment. However, despite several significant exploration campaigns by experienced explorers across a number of prospects, no significant sediment-hosted gold system has yet been discovered in the Gold Hill district.

Krahulec (2017) cites a possible Oligocene mineralizing event based on an unpublished age (AMAX exploration) of the Goshute Wash dike swarm. He defines the dikes as having Climax-type porphyry molybdenum, high-silica rhyolite lithogeochemistry based on high niobium, rubidium, and rubidium over potassium oxide, along with notable molybdenum and tin enrichment. The geochemical support for a porphyry molybdenum system may be valid, but dating in this study places the dike swarm at 16 Ma, notably younger than the Oligocene age. However, the age may still be coincident or only slightly younger than other regional examples of high-silica rhyolites and highly evolved granites such as the Spor Mountain rhyolite and the Sheeprock granite to the east. Also, the age is older than other mineralizing events in the Miocene, primarily the quartz-adularia veins enriched in gold and beryllium that are considered 8 Ma, found in the highest density in the Rodenhouse Wash area (plate 1). Hence, we interpret the Goshute Wash dikes and the Rodenhouse Wash veins as separate mineralizing events occurring within 10 million years of each other and both related to the extension in the Basin and Range during the Miocene.

DESCRIPTION OF MAP UNITS

QUATERNARY-TERTIARY (NEOGENE)

Human-derived Deposits

Qhm **Mining disturbances** (modern to historical) – Areas of disturbed land with waste rock, tailings, and exposures from past (Yellow Hammer, Clifton Shears) and active (Kiewit) mining operations; only large (>330 feet [>100 m]) continuous areas of disturbance are mapped; most past mining operations are associated with minor surface disturbance too small to be reflected on this map; more detail on the numerous historical mining locations in the quadrangle is provided in the Utah Geological Survey's Utah Mineral Occurrence System (UMOS) database and in Robinson (1993); thickness is variable, modern operations such as Keiwit and Yellow Hammer may have over 100 feet (30 m) of waste rock or excavation, whereas historical operations at Clifton Shears are probably less than 50 feet (15 m).

Alluvial Deposits

Qal **Stream alluvium** (Holocene) – Primarily sand, silt, clay and pebble and cobble gravel deposited by streams in channels; grades into alluvium and colluvium in mountain valleys, not mapped separately; locally merges with younger alluvial-fan deposits; locally includes alluvial-fan, colluvial, low-level terrace, lacustrine, and eolian? deposits too small to map separately; thickness generally less than about 20 feet (6 m).

Qafy **Younger fan alluvium** (Holocene to uppermost Pleistocene) – Poorly sorted gravel, sand, silt, and clay; deposited by streams, debris flows, and debris floods on alluvial fans and in mountain valleys; grades to stream alluvium and alluvium and colluvium in mountain valleys; may include small areas of lacustrine fine-grained deposits below the Bonneville shoreline; includes active and inactive fans younger than Lake Bonneville (levels 1 and 2), but may include older alluvial deposits where mapped above the Bonneville shoreline; locally includes eolian silt and sand cover commonly less than 3 feet (1 m) thick; locally, unit Qafy spreads out on lake terraces and abuts Lake Bonneville shorelines even though it is not cut by these shorelines; Qafy also locally drapes over, but does not completely conceal shorelines; thickness variable, up to 50 feet (15 m) or more.

Qafo, Qafo?

Older fan alluvium (upper to middle? Pleistocene) – Poorly sorted gravel, sand, silt, and clay; similar to unit Qafy, but locally cemented with carbonate and forms higher-level incised deposits located above the high stand of Lake Bonneville and locally etched by the lake; incised by younger alluvial deposits; thickness possibly as much as 100 feet (30 m).

Lacustrine Deposits of Lake Bonneville

Ql **Lacustrine deposits, undivided** (upper Pleistocene) – Undivided gravel, sand, silt, marl, and calcareous clay of Lake Bonneville that is interlayered; thin to very thick bedded; may include ostracode- and gastropod-rich layers; locally can include thin eolian silt and sand deposits at surface; mapped in the southeastern part of the quadrangle; locally divided into coarse- and fine-grained deposits (units Qlg and Qlf); Lake Bonneville overview and chronology in Oviatt (2015) and Oviatt and Shroder (2016); thickness as much as 150 feet (45 m) or more.

Qlg **Lacustrine gravel** (upper Pleistocene) – Sandy gravel to boulders composed of rock fragments deposited in shore zones of Lake Bonneville (see Oviatt, 2015 for Lake Bonneville overview and chronology); clasts are typically well rounded and sorted; Lake Bonneville shorelines are locally calcareous tufa-cemented and draped on bedrock (especially at the Provo shoreline); includes both Lake Bonneville transgressive and regressive phase gravels; unit may include small areas of lacustrine sand and fines, eolian silt and sand, and pre-Lake Bonneville alluvial deposits; thinner gravel deposits on bedrock are not mapped; thickness variable, about 100 feet (30 m).

Qlf, Qlf?

Lacustrine fine-grained deposits (upper Pleistocene) – Sand, silt, marl, and calcareous clay of Lake Bonneville; thin to very thick bedded; may include ostracode- and gastropod-rich layers; locally includes small areas of sand or sand and gravel; locally can include thin eolian silt and sand deposits at surface; mapped in the southeastern part of the quadrangle; queried where not field checked; thickness as much as 30 feet (10 m) or more.

Colluvial Deposits

Qc **Colluvium** (Holocene to upper Pleistocene) – Pebble, cobble, and boulder deposits, commonly clast supported, in a matrix of sand, silt, and clay; clasts commonly angular to subangular, but rounded where derived from conglomerates with rounded clasts; unlithified; very poorly sorted, poorly stratified, locally derived; consists of residuum, slope wash, and soil-creep deposits; may include landslides, rockfalls, and debris flows that are too small to map separately; mapped as small cones and debris aprons in drainages and on hillsides; locally contains areas of alluvium not mapped separately; most bedrock is covered by at least a thin veneer of colluvium, but only the larger, thicker deposits are mapped; estimated thickness up to 20 feet (6 m).

Mixed-Environment Deposits

Qla **Lacustrine and alluvial deposits, undivided** (Holocene to upper Pleistocene) – Sand, gravel, silt, and clay; consists of alluvial deposits reworked by Lake Bonneville, lacustrine deposits reworked by streams and covered by slopewash and alluvial fans, as well as alluvial and lacustrine deposits that cannot be readily differentiated at map scale; grades into other lacustrine and alluvial deposits; extensive areas below the Bonneville level shoreline in southeast part of quadrangle; locally includes a thin cover of eolian deposits; thickness up to about 100 feet (30 m) or more.

Stacked-Unit Deposits

Consists of thin surficial deposits covering underlying surficial deposit and bedrock geologic units. See each unit for full descriptions and thickness. Thin unmapped cover materials may also be present on other geologic units throughout the map area.

Qes/Ql **Eolian sand over undivided lacustrine deposits** (Holocene over upper Pleistocene) – Eolian sand and silt overlying Lake Bonneville lacustrine deposits; one area along eastern map border; cover unit thickness as much as 10 feet (3 m).

Ql/Jqm **Undivided lacustrine deposits over Jurassic quartz monzonite** (upper Pleistocene over Late Jurassic) – Lacustrine deposits of Lake Bonneville overlying Jurassic quartz monzonite; Ql has an eolian sand cover in one area (about 0.5 mile [0.8 km] north of Goshute Wash) but not mapped separately; Ql cover is gravelly (with local tufa) in the northeast part of map area, but not mapped separately; cover thickness as much as 10 feet (3 m) or more.

QTaf/Tsc

High-level fan alluvium over Salt Lake Formation conglomerate (lower Pleistocene?-Pliocene? over Miocene) – Upper part (QTaf) of poorly sorted gravel, sand, silt, and clay; somewhat similar to unit Qafo, may be locally cemented with carbonate; clasts up to about 3 feet (1 m) of local sedimentary rocks with carbonate rinds; forms flat-topped, high-level incised deposits located in two areas near North Pass Canyon; lower part of unit (Tsc) is very poorly exposed, light-pink cobble and pebble conglomerate with carbonate matrix; contains dolomite breccia blocks and pods (mapped separately as unit Tbx) that likely represent rock avalanche breccia indicating affinity to the Salt Lake Formation; unit is outboard and adjacent to the eastern range-front fault; alluvial surface is locally about 200 feet (60 m) higher than nearby unit Qafo fan deposits and steps up in elevation to the north; incised by younger alluvial deposits; no direct age control; cover unit thickness uncertain, possibly as much as 300 feet (90 m), and poorly exposed Tsc about 200 feet (60 m).

Unconformity

TERTIARY (NEOGENE-PALEOGENE)

Volcanic rock names were determined through the total alkali-silica (TAS) diagram of the International Union of Geological Sciences Subcommission on the Systematics of Igneous Rocks (IUGS) diagrams (Le Maitre and others, 2002, 2010) and normalized to 100% water-free. See figure 2 and table 1 for more details.

Tj **Jasperoid** (Tertiary?) – Variably colored, but typically dark-red to dark-brown to black jasperoid composed of pervasive silica replacement and iron oxide alteration that obscures primary sedimentary strata; outcrops are dense, resistant and locally brecciated, locally vuggy, and can contain clasts of unaltered rock in a siliceous matrix; typically forms cliffs, knobs, and ledges through the map area; only large (>165 feet [>50 m]) continuous exposures are mapped in the

northern part of the quadrangle; commonly occurs along faults of various ages and orientations, potentially indicating several periods of formation, but chronology is lacking due to difficulty of dating jasperoidal material; Robinson (1993) mapped as breccia (unit bx) in Gold Hill quadrangle; thickness highly variable.

Tsw **Quartz vein stockwork** (Miocene?) - Zone of stockwork quartz-carbonate-adularia veins in strongly oxidized, altered quartz monzonite (granodiorite of Robinson, 2016) and an upper zone of less intense veining and alteration that comprises the Kiewit disseminated gold deposit; in core samples, stockwork consists of randomly oriented to anastomosing veinlets in variably argillic, propylitic, and/or silicified igneous rock; veins are commonly gray, white, and tan and composed of a heterogeneous mix of quartz, chalcedony, calcite, and minor adularia; vein widths commonly less than 1 inch (2 cm) (Robinson, 2016); K-Ar age of 8 Ma on adularia veining event from mine several mi/km north (Whelan, 1970) in the Gold Hill quadrangle; main stockwork zone about 35 to 165 feet (10–50 m) thick and roughly 1000 feet (300 m) across (Robinson, 2016).

Tsc **Salt Lake Formation, conglomerate** (Miocene) – Moderate reddish orange to blood red pebble conglomerate with a sandy to silty matrix; rounded clasts are locally derived from adjoining sedimentary rocks; typically not well indurated; locally red and poorly indurated; also see description of Tsc in unit QTaf/Tsc; locally contains dolomite breccia blocks and pods (mapped separately as unit Tbx) that likely represent rock avalanche breccia similar to the Salt Lake Formation mapped elsewhere (see for example, Miller and others, 1999); located east of the eastern range-front fault and unit QTaf/Tsc exposures, and within a topographic low south of Blood Canyon; Tsc outcrops locally include some unmapped alluvial cover; no age control in map area, but tephrochronology correlation ages of about 9.5 to 13 Ma from Ibapah badlands, Nevada-Utah, west of Deep Creek (Perkins and others, 1998); Salt Lake Formation is equivalent to the Humboldt Formation in Nevada; exposed unit thickness up to about 100 feet (30 m).

Tbx **Dolomite breccia** (Miocene) – Dark-, moderate-, and light-gray dolomite sedimentary breccia (and one area of recrystallized limestone) in blocks and pods within units Tsc and QTaf/Tsc; locally draped by Ql in southeast corner of quadrangle; breccia fragments variable but typically 3 inches (8 cm) or less in diameter of resistant rock avalanche breccia of Paleozoic bedrock units (Guilmette, Laketown, Ely Springs or other); previously mapped by Nolan (1935) as bedrock blocks of Guilmette Formation, Simonson Dolomite?, and Laketown Dolomite; variable and uncertain thickness.

Not in contact

Tid **Igneous dikes, undivided** (Miocene to Oligocene) – Dike swarm near Goshute Wash that cuts southeast side of exposed Jurassic quartz monzonite pluton and one outlier near Overland wash; composition varies from rhyolite to andesite to basalt (geochemical samples GHC22-005, -007, -008) (table 1); differentiation of dike compositions was not possible at map scale; new U-Pb zircon age of 16.23 ± 0.26 Ma on gray to pale green rhyolite porphyry dike (GHC22-010, same outcrop and composition as GHC22-005) (table 2); prior feldspar K-Ar age of 26.6 ± 1.2 Ma on an equivalent composition dike in the same area (Krahulec, 2017) (table 2); overall unit age extent uncertain; dikes up to 100 feet (30 m) thick and approximately 2500 feet (750 m) in length.

Tib **Basalt dikes** (Miocene?) – Dark-gray, weathering to dark-reddish-brown, aphanitic to fine-grained, potassic-trachybasalt dikes; locally vesicular; olivine altered to iddingsite; crops out in a few small, typically bouldery exposures east of Overland Canyon, and also as a minor composition in Goshute Wash dike swarm; previously mapped by Nolan (1935) as part of his unit Tv and by Thomson (1973, plate 3); new geochemical data from samples GHC22-008, -012, -013 (table 1); no age control, but possibly Miocene based on composition and field relation to 16 Ma rhyolite porphyry dike; thickness in Goshute Wash up to 6 inches (20 cm) and as much as 25 feet (8 m) east of Overland Canyon.

Not in contact

Tst **Volcaniclastic sandstone and tuff** (Oligocene? or Eocene?) – Light brownish-gray to pale-red and dark-reddish-brown volcaniclastic sandstone and siltstone and rhyolitic tuff; rocks are water-lain locally with cross-beds, gritty and pebbly lenses of rock fragments and pumice fragments; tuff in Blood Canyon area is low density and reworked; laminated to medium bedded; poorly to well indurated forming slopes and ledges; no age control; exposures in Rodenhouse Wash and near Blood Canyon where it appears to overlie unit Tlf; geochemical data from sample GHC22-003 (table 1); Thomson (1973, plate 3) called these rocks tuff near Blood Canyon; thickness up to 200 feet (60 m).

Tlf **Lava flows** (Oligocene? or Eocene?) – Dark- to moderate-gray and reddish-gray, weathering to dark-reddish-brown and light-brown, porphyritic latite, trachyte and trachydacite lava flows; phenocrysts (~20 percent) of plagioclase, potassium feldspar and hornblende; forms knobs and eroded slopes; exposed in Rodenhouse Wash, northeast of Kiewit mine, northeast margin of Clifton Flat near Gold Hill Wash, and near Blood Canyon; previously mapped by Nolan (1935) as part of unit Tv and as andesite by Thomson (1973, plate 3); new geochemical data from samples GHC22-002, -004, -011 (table 1); no age control, but possibly Oligocene to Eocene based on chemical composition; overlies unit Tt northeast of Clifton Flat; thickness up to about 100 feet (30 m).

Tt **Welded tuff** (Oligocene? or Eocene?) – Light-gray, weathering to dark reddish brown, trachyte to latite welded tuff; phenocrysts (~30 percent) of biotite, hornblende (altered), plagioclase, quartz, potassium feldspar, with some iron oxides and rock fragments; forms resistant knobs and punky pink slopes; exposures along northeast margin of Clifton Flat near Gold Hill Wash; underlies unit Tlf; previously mapped as part of unit Tv by Nolan (1935); new geochemical data from samples GHC22-001, -001a (table 1); no age control, but possibly Oligocene to Eocene based on chemical composition; thickness as much as 80 feet (25 m).

Not in contact

JURASSIC

Plutonic rock names were determined through the total alkali-silica (TAS) diagram of Middlemost (1994) and normalized to 100% water-free. See table 1 and figure 2 for more information.

Jqm, Jqm?

Jurassic quartz monzonite (Late Jurassic) – Pluton of light-gray, weathering to white and reddish brown, biotite-hornblende quartz monzonite that is equigranular to locally porphyritic; medium- to coarsely crystalline, mesocratic to melanocratic, commonly with distinctive pink and violet to light purple alkali feldspars; contains accessory magnetite (with minor ilmenite exsolution lamellae), titanite, zircon, and apatite/fluorapatite; extensive magmatic-hydrothermal alteration is present across the pluton varying from weak to strong and patchy to pervasive; alteration styles include propylitic, potassic, sodic-calcic, sericitization, and argillic alteration with assemblages including bright pink orthoclase altering plagioclase, actinolite altering hornblende, chlorite altering biotite, tourmaline, epidote (including REE endmember allanite), diopside, garnet, ilmenite, apatite, calcite, and scapolite (Nolan, 1935; El Shatoury and Whelan, 1970; Downey, 1976; Burwell, 2018; this study); the pyroxene (augite)-rich monzodiorite identified by Burwell (2018) is interpreted here to be an intense enclave of magmatic-hydrothermal alteration; includes distinct compositional and textural variations such as quartz-rich and quartz-poor phases likely indicating a multiphase (composite) intrusive complex, though high resolution geochronology would be needed to parse the accretion of different phases as multiphase plutons are thought to be formed within ~1–2 million years (e.g., Samperton and others, 2015); crops out over a large part of the northeastern map area where it forms cliffs and slopes; queried in small exposure in Sheep Canyon mapped by Nolan (1935); whole-rock geochemistry based on 15 least-altered pluton samples indicate a quartz monzonite composition (figure 2, table 1), in agreement with data from Burwell (2018); Burwell (2018) also demonstrates that the pluton was emplaced under oxidizing conditions but that oxygen fugacity was likely fluctuating; geochronology with an average biotite K-Ar age of 155 Ma (Stacy and Zartman, 1978; revised using new decay constants) and more recent U-Pb zircon data from Burwell (2018) refine the age to 156.10 ± 1.8 (main phase) and 155.40 ± 1.8 Ma (pyroxene-rich phase) (table 2); the nearby "Granite Mountain" pluton to the east is 150 Ma (Clark and others, 2009, 2016), and other Jurassic plutons in western Utah range from 150 to 170 Ma (Hintze and Kowallis, 2009); thermobarometry from Burwell (2018) identifies the average pressure of the quartz monzonite to be 0.6 kbar, corresponding roughly to an emplacement depth of 1.2 mi (2 km), though the high uncertainty on these calculations calls for further work; thermometry from the same study suggests a range of temperatures from 630° to 990°C, averaging about 750°C, and like the thermobarometry, should be taken with caution given the extensive alteration throughout the pluton; intrusive contact with upper Paleozoic sedimentary units forms a broad alteration zone about 30 to 300 feet (10–100 m) wide, with alteration style and assemblages discussed above; the pluton is cut by the Goshute Wash dike swarm (unit Tid) near Goshute Wash in Clifton Hills; exposed pluton is as much as 20 square mi (50 square km) in the map area, and may extend to the east in the subsurface based on geophysics.

Intrusive contact with Permian, Pennsylvanian, and Mississippian rock units

PERMIAN

Pfm, Pfm(Si), Pfm?

Ferguson Mountain Formation (lower Permian to Upper Pennsylvanian?) – Dark-gray, weathering to light brown, reddish brown and pale red, calcareous siltstone and sandstone with lesser interbedded gray limestone and dolomite; limestone and dolomite can be fossiliferous and cherty; bedding is laminated to thick; forms chippy and platy slopes, ledges, and cliffs; sections are locally poorly exposed and structurally deformed; located at the south end of the Clifton Hills and Blood Mountain and locally in Blood Canyon; unit mapped as the Permian-Pennsylvanian Oquirrh Formation by Nolan (1935), but subsequent stratigraphic studies have revised the nomenclature and report that the upper part of Nolan's Oquirrh Formation in the Gerster Gulch-Gold Hill area contains several middle-lower Permian rock units (see for example, Hose and Reppening, 1959; Bissell, 1962, 1964; Wardlaw and others, 1979); west of Gold Hill, Ferguson Mountain rocks from Twin Peaks into Nevada are apparently part of the hanging wall of the extensive Ferguson detachment sheet (Welsh, 1984; Silberling and Nichols, 2002) and have different lithofacies compared to those in the Clifton quadrangle; Nolan (1935, p. 34) reported thin-bedded platy limestone south and southeast of the Midas mine which contain *Fusulina* (fusulinid fossils) of Pennsylvanian age, but this does not reconcile with recent work in adjoining areas that provides age information from fusulinids (early Leondardian, Wolfcampian, Virgilian, Missourian?) nearby at Twin Peaks (7 miles [11 km] northwest of Gold Hill) (Hodgkinson, 1961; Zabriskie, 1970), near the Owl Hills No. 1 well NV (Bissell, 1964), and the type section at Ferguson Mountain, Nevada (Berge, 1960; Steele, 1959; 1960; Slade, 1961; Stevens and others, 1979); originally called the Ferguson Springs Formation (Steele, 1959, 1960) and subsequently revised to the Ferguson Mountain Formation (Berge, 1960; Slade, 1961); formation may unconformably overlie the Ely Limestone in the map area, and no Strathearn Formation was noted at southern Blood Mountain (for nearby areas see Hodgkinson, 1961; Bissell, 1964; Zabriskie, 1970); queried in exposures near Overland wash that could be Ely Limestone; (Si) added to map symbol where exposures are silicified; incomplete thickness is about 1745 feet (532 m) at southern Blood Mountain and uncertain thickness south of the Jurassic pluton and Midas fault; 1715 feet (525 m) reported at Twin Peaks (incomplete?) (Hodgkinson, 1961; Zabriskie, 1970); complete thickness of 2200 to 3095 feet (670–945 m) measured at type sections in Nevada but uncertain lower contact issues noted (see Steele, 1959, 1960; Berge, 1960; Hodgkinson, 1961; Slade, 1961; Bissell, 1962).

Unconformity?

PENNSYLVANIAN-MISSISSIPPIAN

IPe, IPe?

Ely Limestone (Middle-Lower Pennsylvanian to uppermost Mississippian) – Moderate-gray to blue-gray limestone and dolomite with lesser sandy limestone, and interbedded light-brown-weathering dark-gray calcareous siltstone and sandstone; locally thin light-brown sandstone interbeds and wispy sand; locally cherty (gray and black) and fossiliferous (brachiopods, bryozoa, echinoderms, corals, fusulinids); bedding is thin to very thick; cyclic character that forms cliffs, ledges, slopes around the perimeter of Clifton Flat, and Blood Canyon and Blood Mountain areas; locally can be difficult to differentiate from the Ochre Mountain Limestone, particularly in structurally complex areas; Robinson (1993) reported that Ely exposures to the north have a greater percentage of sandstone that exceeds the carbonate rocks; macrofossils, fusulinids, and conodonts are reported from the formation in the Gold Hill district (Nolan, 1935; Harris in Robinson, 1993); some collections of Nolan (1935) are reported to contain *Fusulina* (fusulinid) (now considered Middle and Early Pennsylvanian age); Middle-Early Pennsylvanian fusulinids are reported from equivalent strata nearby in Nevada (Slade, 1961, Bissell, 1964) and lower extent from Sadlick (1965); in part corresponds to Nolan's (1935) Oquirrh Formation, but subsequent studies revised the age and nomenclature, yet we do not use the terminology of Bissell (1964); Ely Limestone typically underlies a regional Upper-Middle Pennsylvanian unconformity; locally queried where uncertain affinity; Ely is underlain by the slope-forming Chainman Formation, contact is conformable or locally faulted; incomplete exposed thickness is about 2160 to 3520 feet (659–1073 m) at northern Blood Mountain and south of Uiyabi Canyon; roughly 1400 feet (425 m) thick in the Gold Hill quadrangle (Robinson, 1993).

MISSISSIPPIAN

Mc **Chainman Formation** (Upper Mississippian) – Black to gray fissile shale with interbedded gray fine-grained quartzite and sandstone, and dark-gray to black micritic limestone; weathered surfaces are commonly stained light red-

dish brown, dark red, and black; bedding is laminated to medium; forms slopes and some ledges; the formation is considered Chesterian in age from macrofossils at Gold Hill and regionally (Nolan, 1935; Sadlick, 1965); this mechanically weak formation has been highly deformed and attenuated by multiple structural events (Nolan, 1935; Robinson, 1993); Christiansen (1975) reports on contact metamorphism of the unit associated with the Gold Hill Jurassic pluton; crops out in limited exposures along the Ochre Mountain thrust fault, in Rodenhouse Wash, Blood Canyon, and along faults and the intrusive contact near Overland Canyon; contact with underlying Ochre Mountain Formation may be conformable or faulted?; previously mapped by Nolan (1935) as the Manning Canyon Shale; to the north, other areas in northwest Utah have been mapped as the Diamond Peak Formation and Chainman Shale, undivided (Miller and others, 2020, 2021), but the Diamond Peak may not extend south to the Gold Hill area (Sadlick, 1965; Rose, 1976; Silberling and others, 1997); incomplete exposed thickness as much as 450 feet (140 m) near the Midas mine (south of Montezuma Peak) (Nolan, 1935).

Mo, Mo?

Ochre Mountain Limestone (Upper Mississippian) – Dark-blue to blue-gray limestone that is locally cherty and fossiliferous; limestone is finely crystalline with micritic to coarse-grained beds; includes minor interbeds of fine-grained quartz arenite, and shale which weathers pinkish red or pale yellow; locally includes a dark-colored shale interval (unit Mos) mapped separately and described below; limestone with common and locally abundant stringers of light-gray and black chert, mostly less than 3 inches (7.5 cm) thick, particularly in the lower part of the unit; thick to very thick bedded; forms cliffs and ledges; outcrops are locally highly fractured and riddled with calcite veins; intraformational breccias, probably of tectonic origin based on the lack of conformity of breccias with bedding, occur throughout the unit; bleaching and silicic alteration alter the appearance of the limestone in many locations (Robinson, 1993); Ochre Mountain Limestone can be very difficult to differentiate from the Ely Limestone, particularly in structurally complex areas, we assigned darker-colored and chertier rocks to the Ochre Mountain; Chamberlain (1981) and Harmala (1982) conducted biostratigraphic studies in the Gold Hill quadrangle that indicate the formation is incomplete, and a section in the extreme southwest corner of the quadrangle yielded Chesterian-Meramecian fossils (Chamberlain, 1981); considered correlative to the Great Blue Limestone of central Utah (Nolan, 1935; Chamberlain, 1981; Hintze and Kowallis, 2009); conformable contact with the underlying Woodman Formation is mapped near the northwest corner of the Clifton quadrangle; Robinson (1993) reports that to the north, the lower contact of the formation is commonly a sub-horizontal fault, either the Ochre Mountain thrust or a low-angle normal fault; incomplete, exposed thickness is uncertain but <1050 feet (320 m) measured by Harmala (1982) at Ochre Mountain to the northwest; roughly 1475 feet (450 m) in the Gold Hill quadrangle (Robinson, 1993), and 470 feet (145 m) at northern Dugway Range (Staatz and Carr, 1964).

Mos **Ochre Mountain Limestone, shale member** (Upper Mississippian) – Dark gray to black shale with thin sandstone lenses mapped within the Ochre Mountain Limestone and called the Herat shale member by Nolan (1935); bedding is laminated to thin and forms slopes; crops out near Blood Canyon and Clifton, where mapped as a marker bed; Nolan (1935) reported unit is similar in appearance to the Manning Canyon Shale [Chainman], and mapped at Ochre Mountain, Blood Canyon, and north and west of Clifton; Nolan (1935) noted bedding-parallel slip and attenuation in many exposures; Harmala (1982) measured sections at nearby Ochre Mountain and obtained Chesterian and Osagean fossils from strata of the underlying Ochre Mountain Limestone (also see Poole and Sandberg, 1991), and he indicated uncertainty about the shale's stratigraphic position considering the structural complexity there, and noted that the Herat shale member remained problematic and may be the base of the Manning Canyon Formation [Chainman] in the area; considering the above, we use an informal member designation for the shale interval; thickness is up to 50 feet (15 m) (Nolan, 1935).

Mw **Woodman Formation** (Upper-Lower Mississippian) – Light-brown to light-gray, platy, calcareous siltstone and sandstone, and dark-gray sandy, micritic limestone; bedding is laminated to thick; forms slopes and ledges; upper part crops out north of Clifton Flat in northwest part of map area; lower part of the Woodman Formation near Gold Hill includes the Needle Siltstone Member and Delle Phosphatic Member (Harmala, 1982; Sandberg and Gutschick, 1984; Poole and Sandberg, 1991; Robinson, 1993); age is Meracecian and Osagean in the northern Deep Creek Mountains, and Woodman correlates to the Humbug Formation (part or none) and Deseret Limestone of north-central Utah (Poole and Sandberg, 1991); incomplete, exposed thickness is uncertain, but Nolan (1935) estimated <1500 feet (457 m); incomplete estimated thickness of 1180 feet (360 m) in adjacent quadrangle (Robinson, 1993), and other thicknesses are 445 feet (135 m) in the southern Lakeside Mountains (Silberling and Nichols, 1992) and 786 feet (240 m) in the northern Dugway Range (Staatz and Carr, 1964).

Not in contact

DEVONIAN

Dsi? **Simonson Dolomite?** (Middle Devonian) – Single exposure of light-, moderate- and dark-gray dolomite that is medium bedded and forms ledges; locally brecciated and silicified; faulted exposure along west map border adjacent to the Christiansen Canyon fault; queried due to lack of lamination and faulted stratigraphic context; Nolan (1935) called this exposure Simonson Dolomite and reported on intact sections and fossils nearby; incomplete thickness roughly 200 feet (60 m); about 1000 feet (300 m) thick in surrounding areas (Nolan, 1935).

Fault

SILURIAN

Sl? **Laketown Dolomite?** (Silurian) – Single area of light-moderate-gray to light-bluish-gray dolomite that is medium to thick bedded and forms resistant knobs and cliffs; faulted exposure along west map border adjacent to the Christiansen Canyon fault; queried due to faulted stratigraphic context; Nolan (1935) called this exposure Laketown Dolomite and reported on lithologic sections and coral collections nearby; incomplete thickness as much as 570 feet (175 m); complete thickness in area is 970 feet (295 m) (Nolan, 1935).

Fault

CAMBRIAN

Cambrian rock units are exposed in a west-dipping structural block of the northern Deep Creek Mountains. The upper part of the Cambrian section is west of the map area. Nolan (1935), Bick (1966), Kepper (1969), and Thomson (1973) used Cambrian stratigraphic nomenclature that has been superseded by that of McCollum and McCollum (1984) which better meshes with regional nomenclature (see for example, Hintze and Robison, 1975; McCollum and Miller, 1991; Hintze and Davis, 2003).

Ꞓl, Ꞓl? **Lamb Dolomite** (Upper-Middle? Cambrian) – Typically gray-colored dolomite and limestone; upper part (150 feet [45 m]) is thin bedded, silty dolomite and limestone with about 40 feet (12 m) of reddish-weathering fine-grained sandstone at the top; middle part is light to medium gray dolomite with darker mottling, contains white rods of dolomite and calcite, medium to thick bedded; lower part is light-gray dolomite that is oolitic and pisolitic and very thick bedded; forms cliffs, ledges and slopes; locally queried near the Christiansen Canyon fault where altered and incomplete; trilobites from the upper part are *Crepicephalus* (Bick, 1966; McCollum and McCollum, 1984); lower contact marked by a change from oolitic dolomite to underlying limestone and shale of the Trippe Limestone; only lower part present in quadrangle, about 460 feet (140 m) thick; complete thickness nearby is 800 to 1050 feet (245–320 m) (Nolan, 1935; Kepper, 1969; McCollum and McCollum, 1984), Bick measured 1162 feet (354 m) to the south.

Ꞓtl **Trippe Limestone** (Middle Cambrian) – Gray to light-brown limestone and dolomite that is locally oolitic with intraformational conglomerate; bedding is typically thin; forms cliffs, ledges and slopes; shaley upper part containing *Eldoradia* trilobites and reportedly corresponds to the Fish Springs Member (Hintze and Robison, 1974 unpublished data; McCollum and McCollum, 1984), not mapped separately; lower contact is sharp, marked by change from cherty dolomite of unit Ꞓtl to dark dolomite of the Young Peak dolomite; complete thickness is 660 to 765 feet (180–235 m) (Nolan, 1935, Kepper, 1969; McCollum and McCollum, 1984); Bick reports 795 feet (242 m) to the south.

Ꞓpy, Ꞓpy?

"Pierson Cove" Formation, Young Peak dolomite member (Middle Cambrian) – Dark gray dolomite with white dolomite rods that is thin to thick bedded; locally oolitic and mottled; forms cliffs and ledges; distinctive dolomite unit that is mapped separately from the carbonate-shale sequence above and below; McCollum and McCollum (1984) include it as a dolomitic lithosome within the limestone of the upper "Pierson Cove" Formation (tentative assignment), but say it is a local unit with no regional value; previously mapped as the Young Peak dolomite by Nolan (1935) and Bick (1966); lower contact climbs and interfingers with Pierson Cove limestone northward; contains *Bolaspidella* trilobite fauna (McCollum and Miller, 1991); complete thickness up to about 600 feet (180 m) (Nolan, 1935; Kepper, 1969; McCollum and McCollum, 1984); Bick (1966) measured about 350 feet (105 m) to the south.

Ꞓph, Ꞓph?

"Pierson Cove" through Howell Formations, undivided (Middle Cambrian) – Combined unit that consists of (descending) the "Pierson Cove" Formation (tentative assignment), Wheeler Shale, Swasey Limestone, Whirlwind Formation, Dome Limestone, Chisholm Shale, and Howell Formation (after McCollum and McCollum, 1984), formerly the Abercrombie Formation of Nolan (1935); typically gray to brown silty limestone and interbedded shale, limestone locally dolomitized; bedding is laminated to thick; unit forms ledges, slopes and cliffs; mapped where formations are difficult to separate due to similar lithologies, local exposure, vegetation, and faulting; several types of diagnostic trilobites are reported from this section (see McCollum and McCollum, 1984); sharp lower contact marked by change from Howell limestone to Busby Quartzite Member of the Pioche Formation; sections in Dry and Sheep Canyons were measured by Nolan (1935), Kepper (1969), and L.F. Hintze and R.A. Robison (1974 unpublished); Hintze and Robison (1974 unpublished) also noted difficulty in separating the various units of this interval; complete thickness is about 2500 to 2700 feet (760–825 m) (Nolan, 1935; Kepper, 1969 [reported less]; Hintze and Robison, 1974 unpublished; McCollum and McCollum, 1984); Bick (1966) measured 1765 feet (540 m) in Goshute Canyon to the south.

Ꞓpib **Pioche Formation, Busby Quartzite Member** (Middle-Lower? Cambrian) – Brown quartzite and sandstone with lesser shale beds (similar to the Cabin Member); a rust-colored (dark-gray fresh) dolomite bed (about 3 feet [1 m] thick) is present in the upper part of the unit (similar to Tatow Member to the east and south); thin to thick bedded; forms cliffs, ledges and slopes; sparse trilobites reported by A.R. Palmer in Bick (1966); Hintze and Kowallis (2009) show *Olenellus* trilobite zone in this unit; lower contact is gradational and placed at the change from quartzite to underlying shale of Cabin Shale Member; thickness in the area ranges from about 410 to 450 feet (125–135 m) (Nolan, 1935; Bick, 1966; Rodgers, 1989).

Ꞓpic **Pioche Formation, Cabin Shale Member** (Lower Cambrian) – Dark-brown, green and red shale and siltstone that is micaceous and becomes sandy near top of unit; bedding is laminated; typically forms slopes; contains *Olenellus* (trilobite) (McCollum and McCollum, 1984); lower contact marked by a sharp transition from recessive shale to resistant, cliff-forming quartzite of the Prospect Mountain Quartzite; thickness is about 500 feet (150 m) (Nolan, 1935, Rodgers, 1989).

CAMBRIAN-NEOPROTEROZOIC?

ꞒZpm **Prospect Mountain Quartzite** (Lower Cambrian to Neoproterozoic?) – Brown to light-brown quartzite and sandstone that is medium to thick bedded; commonly fine to medium grained, but coarser-grained lenses are also present, and commonly cross-bedded; locally contains sporadic quartz pebble conglomerates and few shaley beds; forms resistant cliffs and ledges; lower contact not exposed in the quadrangle; incomplete thickness in the map area is about 800 feet (245 m) (Nolan, 1935), but the total thickness of the unit is estimated at 3000 feet (915 m) or greater (Nolan, 1935; Rodgers, 1989) and Bick reported 2950 feet (900 m) in Goshute Canyon to the south.

ACKNOWLEDGMENTS

This geologic map and associated GIS work on the adjacent Gold Hill quadrangle (Robinson, 2023) was funded by the U.S. Geological Survey through Earth MRI award number G20AC00168 (2020–22). We thank mine and property owners for access to the area. Jamie Robinson (Dumont Nickel), Jeff Nichols and Eric Lauha (formerly Newmont Gold), and Ken Krahulec (UGS retired) provided historical knowledge and geologic expertise. We thank Newmont Gold for providing proprietary aeromagnetic data. Nathan Carey and Simon Jowitt (University of Nevada, Las Vegas) conducted petrographic evaluations in cooperation with this project. USGS and ALS Global performed geochemical analyses of igneous rocks. Current and former UGS staff including Taylor Boden, Kayla Smith, Will Hurlbut, and Bear Jordan assisted in the field and office. UGS reviewers Zachary Anderson, Stefan Kirby, Stephanie Carney, and Michael Hylland improved this map product. UGS staff Jen Miller and Lori Steadman assisted with preparation of the explanatory materials, and Rosemary Fasselin and Subigya Shah organized the GIS and GeMS data.

REFERENCES

Armstrong, R.L., 1970, Geochronology of Tertiary igneous rocks, eastern Basin and Range Province, western Utah eastern Nevada and vicinity, U.S.A.: Geochimica et Cosmochimica Acta, v. 34, p. 205–232.

Berge, J.S., 1960, Stratigraphy of the Ferguson Mountain area, Elko County, Nevada: Brigham Young University Research Studies, v. 7, no. 5, 63 p., 2 plates.

Best, M.G., and Christiansen, E.H., 1991, Limited extension during peak Tertiary volcanism, Great Basin of Nevada and Utah: Journal of Geophysical Research, v. 96, p. 13,509–13,528.

Bick, K.F., 1966, Geology of the Deep Creek Mountains, Tooele and Juab Counties, Utah: Utah Geological and Mineralogical Survey Bulletin 77, 120 p., 2 plates, map scale 1:66,172, https://doi.org/10.34191/B-77.

Bissell, H.J., 1962, Permian rocks of part of Nevada, Utah, and Idaho: GSA Bulletin, v. 73, p. 1083–1110.

Bissell, H.J., 1964, Ely, Arcturus, and Park City Groups (Pennsylvanian-Permian) in eastern Nevada and western Utah: American Association of Petroleum Geologists Bulletin, v. 48, p. 565–636.

Burwell, J., 2018, Alteration and associated mineralization in the Gold Hill Jurassic pluton, Tooele County, Utah: Tucson, University of Arizona, M.S. thesis, 186 p.

Butler, B.S., Loughlin, G.F., and Heikes, V.C., 1920, The ore deposits of Utah: U.S. Geological Survey Professional Paper 111, 672 p.

Chamberlain, A.K., 1981, Biostratigraphy of the Great Blue Formation: Brigham Young University Geology Studies, v. 28, part 3, p. 9–17.

Carey, N.J., 2022, Age and genesis of W-Mo-Cu mineralization, Gold Hill, Utah: Las Vegas, University of Nevada, M.S. thesis, 143 p.

Chen, C.Y., and Maloof, A.C., 2017, Revisiting the deformed high shoreline of Lake Bonneville: Quaternary Science Reviews, v. 159, p. 169–189.

Chorney, R., 1943, Scheelite and the mineral association at the Reaper mine, Gold Hill, Utah: Salt Lake City, University of Utah, M.S. thesis, 47 p.

Christensen, O.D., 1975, Metamorphism of the Manning Canyon and Chainman Formations: Stanford, California, Stanford University, Ph.D. dissertation, 166 p.

Christiansen, R.L., and McKee, E.H., 1978, Late Cenozoic volcanic and tectonic evolution of the Great Basin and Columbia intermontane regions: Geological Society of America Memoir 152, p. 283–311.

Clark, D.L., 2020, The Uinta-Tooele structural zone—what's in a name?: Utah Geological Survey, Survey Notes, v. 52, no. 2, p. 4–5, https://doi.org/10.34191/SNT-55-2.

Clark, D.L., Biek, R.F., Willis, G.C., Brown, K.D., Kuehne, P.A., Ehler, J.B., and Ege, C.L., 2009, Geologic map of the Granite Peak and Sapphire Mountain area, U.S. Army Dugway Proving Ground, Tooele County, Utah: Utah Geological Survey Map 238, 2 plates, scale 1:24,000, https://doi.org/10.34191/M-238.

Clark, D.L., Oviatt, C.G., and Page, D., 2016, Geologic map of Dugway Proving Ground and adjacent areas, Tooele County, Utah: Utah Geological Survey Map 274DM, 31 p., 2 plates, scale 1:75,000, https://doi.org/10.34191/M-274dm.

Currey, D.R., 1982, Lake Bonneville—selected features of relevance to neotectonic analysis: U.S. Geological Survey Open-File Report 82-1070, 30 p., 1 plate, scale 1:500,000.

Dalrymple, G.B., 1992, Critical tables for conversion of K-Ar ages from old to new constants: Isochron/West, Bulletin of Isotopic Geochronology, v. 58, p. 22-24.

DeCelles, P.G., 2004, Late Jurassic to Eocene evolution of the Cordilleran thrust belt and foreland basin system, western U.S.A.: American Journal of Science, v. 304, p. 105–168.

Downey, L.M., 1976, Geochemistry of hydrothermal chlorites, Gold Hill, Utah: Salt Lake City, University of Utah, M.S. thesis, 65 p.

El-Shatoury, H.M., 1967, Mineralization and alteration studies in the Gold Hill mining district: Salt Lake City, University of Utah, Ph.D. dissertation, map scale 1:600.

El-Shatoury, H.M., and Whelan, J.A., 1970, Mineralization in the Gold Hill mining district, Tooele County, Utah: UGMS Bulletin 83, 37 p., 3 plates.

Harmala, J.C., 1982, Conodont biostratigraphy of some Mississippian rocks in northeastern Nevada and northwestern Utah: Tempe, Arizona State University M.S. thesis, 271 p.

Hintze, L.F., and Davis, F.D., 2003, Geology of Millard County, Utah: Utah Geological Survey Bulletin 133, 305 p., https://doi.org/10.34191/B-133.

Hintze, L.F., and Kowallis, B.J., 2009, Geologic history of Utah: Brigham Young University Geology Studies Special Publication 9, 225 p.

Hintze, L.F., and Robison, R.A., 1975, Middle Cambrian stratigraphy of the House, Wah Wah, and adjacent ranges in western Utah: Geological Society of America Bulletin, v 86, p. 881–891.

Hodgkinson, K.A., 1961, Permian stratigraphy of northeastern Nevada and northwestern Utah: Brigham Young University Geology Studies, v. 8, p. 167–196.

Hose, R.K., and Reppening, C.A., 1959, Stratigraphy of Pennsylvanian, Permian, and Lower Triassic rocks of Confusion Range, west-central Utah: American Association of Petroleum Geologists Bulletin, v. 43, p. 2167–2196.

International Commission on Stratigraphy, International Chronostratigraphic Chart v 2023/04: Online, https://stratigraphy.org/ICSchart/ChronostratChart2023-04.pdf, accessed April 17, 2023.

Kepper, J.C., 1969, Stratigraphy and petrology of a Middle and Upper Cambrian interval in the Great Basin: Seattle, University of Washington, Ph.D. thesis, 251 p.

King, C.A., and Burwell, J., 2016, Report on the igneous petrology and U-Pb ages of igneous rocks from Gold Hill and Ferber Flats geochronology of the igneous rocks: Unpublished Report by the University of Arizona, Tucson, Arizona,16 p.

Krahulec, K., 2017, Mineral resource potential of the Gold Hill mining district, Tooele County, Utah: Utah Geological Survey Contract Deliverable to the School and Institutional Trust Lands Administration, 63 p.

Le Maitre, R.W., Streckeisen, A., Zanettin, B., Le Bas, M.J., Bonin, B., Bateman, P., 2002, online version 2010, Igneous rocks–a classification and glossary of terms: Recommendations of the International Union of Geological Sciences Subcommission on the Systematics of Igneous Rocks, 2nd Edition, Cambridge University Press, doi.org/10.1017/CBO9780511535581.

Malan, P.O., 1989, Geology of the southern half of the Gold Hill Mining District, Tooele County, Utah: Pocatello, Idaho State University, M.S. thesis, 75 p., 2 plates, map scale 1:24,000.

McCollum, L.B., and McCollum, M.B., 1984, Comparison of a Cambrian medial shelf sequence with an outer shelf margin sequence, northern Great Basin, *in* Kerns, G., and Kerns, R.L., Jr., editors, Geology of northwest Utah, southern Idaho and northeast Nevada: Utah Geological Association Publication 13, p. 35–44.

McCollum, L.B., and Miller, D.M., 1991, Cambrian stratigraphy of the Wendover area, Utah and Nevada: U.S. Geological Survey Bulletin 1948, 43 p.

Middlemost, E.A.K.,1994, Naming materials in the magma/igneous rock system: Earth-Science Reviews, v. 37, no. 3-4, p. 215–224.

Miller, D.M., 1990, Mesozoic and Cenozoic tectonic evolution of the northeastern Great Basin, *in* Buffa, R.H., and Coyner, A.R., editors, Geology and ore deposits of the Great Basin: Field trip guidebook compendium, volume 1, Great Basin Symposium 1990, Geological Society of Nevada and the U.S. Geological Survey, p. 202–228.

Miller, D.M., Clark, D.L., Wells, M.L., Oviatt, C.G., Felger, T.J., and Todd, V.R., 2020, Interim geologic map of the Grouse Creek and Utah part of the Jackpot 30' x 60' quadrangles, Box Elder County, Utah, and Cassia County, Idaho: Utah Geological Survey Open-File Report 716DM, 31 p., 1 plate, scale 1:62,500, https://doi.org/10.34191/OFR-716dm.

Miller, D.M., Felger, T.J., and Langenheim, V.E., 2021, Geologic and geophysical maps of the Newfoundland Mountains and part of the adjacent Wells 30' x 60' quadrangles, Box Elder County, Utah: Utah Geological Survey Miscellaneous Publication 173DM, 26 p., 2 plates, scale 1:62,500, https://doi.org/10.34191/MP-173dm.

Miller, D.M., and Hoisch, T.D., 1995, Jurassic tectonics of northeastern Nevada and northwestern Utah from the perspective of barometric studies, *in* Miller, D.M., and Busby, C., editors, Jurassic magmatism and tectonics of the North American Cordillera: Boulder, Colorado, Geological Society of America Special Paper 299, p. 267–294.

Miller, E.L., Dumitru, T.A., Brown, R.W., and Gans, P.B., 1999, Rapid Miocene slip on the Snake Range-Deep Creek Range fault system, east-central Nevada: Geological Society of America Bulletin, v. 111, no. 6, p. 889–905.

Mills, S.E., in progress, Mineral and geochemical report for the Gold Hill district, Utah (tentative authorship and title): Utah Geological Survey Open-File Report.

Moore, W.J., and McKee, E.H., 1983, Phanerozoic magmatism and mineralization in the Tooele 1x2-degree quadrangle, Utah: Geological Society of America Memoir 157, p. 183–190.

Nolan, T.B., 1935, The Gold Hill mining District, Utah: U.S. Geological Survey Professional Paper 177, 172 p., 3 plates, geologic map scales 1:62,500 (plate 1) and 1:24,000 (plate 2), structure map (plate 3).

Oviatt, C.G., 2015, Chronology of Lake Bonneville, 30,000 to 10,000 yr B.P.: Quaternary Science Reviews, v. 110, p. 166–171.

Oviatt, C.G., and Shroder, J., editors, 2016, Lake Bonneville—a scientific update—Developments in earth surface processes, v. 20: Elsevier, 659 p.

Perkins, ME., Brown, F.H., Nash, W.P. McIntosh, W., and Williams, S.K., 1998, Sequence, age, and source of silicic fallout tuffs in middle to late Miocene basins of the northern Basin and Range Province: Geological Society of America Bulletin, v. 110, no. 3, p. 344–360.

Poole, F.G., and Sandberg, C.A., 1991, Mississippian paleogeography and conodont stratigraphy of the western United States, *in* Cooper, J.D., and Stevens, C.H., editors, Paleozoic paleogeography of the western United States II: Los Angeles, Pacific Section, Society of Economic Paleontologists and Mineralogists, v. 1, p. 107–136.

Roberts, R.J., Crittenden, M.D., Tooker, E.W., Morris, H.T., Hose, R.K., and Cheney, T.M., 1965, Pennsylvanian and Permian basins in northwestern Utah and northeastern Nevada and south-central Idaho: American Association of Petroleum Geologists Bulletin, v. 40, no. 11, p. 1926–1956.

Robinson, J.P., 1990, A comprehensive study of the structural geology and regional tectonics of the Gold Hill area, northern Deep Creek Mountains, western Utah: Ithaca, N.Y., Cornell University, Ph.D. dissertation, 287 p.

Robinson, J.P., 1993, Provisional geologic map of the Gold Hill quadrangle, Tooele County, Utah: Utah Geological Survey Map 140, 16 p., 3 plates, scale 1:24,000. [plate 3: Mines, Prospects, and Workings of the Gold Hill quadrangle by H.M. Messenger, H.H. Doelling, B.T. Tripp, and M.E. Jensen], https://doi.org/10.34191/M-140.

Robinson, J.P., 2006, Gold Hill, Utah—polyphase, polymetallic mineralization in a transverse zone, *in* Bon, R.L., Gloyn, R.W., and Park, G.M., editors, Mining districts of Utah: Utah Geological Association Publication 32, p. 167–182.

Robinson, J.P., 2016, The Kiewit gold deposit—A late Miocene (?) low-sulfidation gold-quartz stockwork, Gold Hill mining district, Tooele County, Utah, *in* Comer, J.B., Inkenbrandt, P.C., Krahulec, K.A., and Pinnell, M.L., editors, Resources and geology of Utah's West Desert: Utah Geological Association Publication 45, p. 43–58.

Robinson, J.P., 2023, Provisional geologic map of the Gold Hill quadrangle, Tooele County, Utah (GIS Reproduction of UGS Map 140 [1993]): Utah Geological Survey Map 301DR, 20 p., 3 plates, scale 1:24,000., scale 1:24,000, https://doi.org/10.34191/M-301DR.

Rodgers, D.W., 1987, Thermal and structural evolution of the southern Deep Creek Range, west central Utah and east central Nevada: Stanford, California, Stanford University, Ph.D. dissertation, 149 p., map scale 1:50,000.

Rodgers, D.W., 1989, Geologic map of the Deep Creek Mountains Wilderness Study Areas, Tooele and Juab Counties, Utah: U.S. Geological Survey Miscellaneous Field Studies Map MF-2099, scale 1:50,000.

Rose, P.R., 1976, Mississippian carbonate shelf margins, western United States, *in* Hill, J.G., editor, Geology of the Cordilleran hingeline: Rocky Mountain Association of Geologists – 1976 Symposium, p. 135–151.

Sadlick, W., 1965, Biostratigraphy of the Chainman Formation, eastern Nevada and western Utah: Salt Lake City, University of Utah, Ph.D. dissertation, 227 p.

Samperton, K.M., Schoene, B., Cottle, J.M., Keller, C. Brenhin, Crowley, J.L., and Schmitz, M.D., 2015, Magma emplacement, differentiation and cooling in the middle crust—Integrated zircon geochronological-geochemical constraints from the Bergell Intrusion, central Alps: Chemical Geology, v. 417, p. 322–340, https://doi.org/10.1016/j.chemgeo.2015.10.024.

Sandberg, C.A., and Gutschick, R.C., 1984, Distribution, microfauna, and source-rock potential of Mississippian Delle Phosphatic Member of Woodman Formation and equivalents, Utah and adjacent states, *in* Woodward, J., Meissner, F.F., and Clayton, J.L., editors, Hydrocarbon source rocks of the Greater Rocky Mountain region: Denver, Colorado, Rocky Mountain Association of Geologists, p. 137–178.

Silberling, N.J., Nichols, K.M, Trexler, J.H., Jr., Jewell, P.W., and Crosbie, R.A., 1997, Overview of Mississippian depositional and paleotectonic history of the Antler foreland, eastern Nevada and western Utah: Brigham Young University Geology Studies, v. 42, part 1, p. 161–196.

Silberling, N.J., and Nichols, K.M., 1992, Depositional cycles of the Upper Devonian-Lower Mississippian Limestone succession in the southern Lakeside Mountains, Utah, with an appendix on the identification and age interpretations of conodont faunas by R.G. Stamm, *in* Wilson, J.R., editor, Field guide to geologic excursions in Utah and adjacent areas of Nevada, Idaho, and Wyoming, prepared for the Geological Society of America Rocky Mountain Section meeting in Ogden, Utah, May 13–15, 1992: Utah Geological Survey Miscellaneous Publication 92-3, p. 131–145, https://doi.org/10.34191/MP-92-3.

Silberling, N.J., and Nichols, K.M., 2002, Geologic map of the White Horse Pass area, Elko County, Nevada: Nevada Bureau of Mines and Geology Map 132, 8 p., 1 sheet, scale 1:24,000.

Slade, M.L., 1961, Pennsylvanian and Permian fusulinids of the Ferguson Mountain area, Elko County, Nevada: Brigham Young University Geology Studies, v. 8, p. 55–94.

Staatz, M.H., and Carr, W.J., 1964, Geology and mineral deposits of the Thomas and Dugway Ranges, Juab and Tooele Counties, Utah: U.S. Geological Survey Professional Paper 415, 188 p.

Stacy, J.S., and Zartman, R.E., 1978, A lead and strontium isotopic study of igneous rocks and ores from the Gold Hill mining district, Utah: Utah Geology, v. 5, p. 1–15.

Steele, G., 1959, Stratigraphic interpretation of the Pennsylvanian-Permian systems of the eastern Great Basin: Seattle, University of Washington, Ph.D. dissertation, 264 p.

Steele, G., 1960, Pennsylvanian-Permian stratigraphy of east-central Nevada and adjacent Utah: Intermountain Association of Petroleum Geologists Guidebook 11th Annual Field Conference, p. 91–113.

Stevens, C.H., Wagner, D.B., and Sumsion, R.S., 1979, Permian fusulinid biostratigraphy, central Cordilleran miogeosyncline: Journal of Paleontology, v. 53, no. 1, p. 29–36.

Thomson, K.C., 1973, Mineral deposits of the Deep Creek Mountains, Tooele and Juab Counties, Utah: Utah Geological and Mineralogical Bulletin 99, 76 p., 8 plates, https://doi.org/10.34191/B-99.

U.S. Geological Survey, 2023, Geochronology database: Online, https://apps.usgs.gov/geochron_database_explorer/, accessed May 2, 2023.

Utah Geological Survey, 2023, Quaternary fault map: Online, https://geology.utah.gov/apps/hazards/, accessed March 3, 2023.

Wardlaw, B.R., Collinson, J.W., and Maughan, E.K., 1979, Stratigraphy of Park City Group equivalents (Permian) in southern Idaho, northeastern Nevada, and northwestern Utah, *in* Wardlaw, B.R., editor, Studies of Permian Phosphoria Formation and related rocks, Great Basin-Rocky Mountain region: U.S. Geological Survey Professional Paper 1163-C, p. 9–16.

Wernicke, B., and Burchfiel, B.C., 1982, Modes of extensional tectonics: Journal of Structural Geology, v. 4, issue 2, p. 105–115, https://doi.org/10.1016/0191-8141(82)90021-9.

Welsh, J.E., 1984, Field trip day 2 road log–West Wendover, Nevada through Ferguson Flat to Gold Hill, Utah, *in* Kerns, G.J, and Kerns, R.L., editors, Geology of northwest Utah, southern Idaho and northeast Nevada: Utah Geological Association Publication 13, p. 275–276.

Whelan, J.A., 1970, Radioactive and isotopic age determinations of Utah rocks: Utah Geological and Mineralogical Survey Bulletin 81, 75 p., https://doi.org/10.34191/B-81.

Yonkee and Weil, 2015, Tectonic evolution of the Sevier and Laramide belts within the North American Cordilleran orogenic system: Earth-Science Reviews, v. 150, p. 531–593, http://dx.doi.org/10.1016/j.earscirev.2015.08.001.

Zabriskie, W.E., 1970, Petrology and petrography of Permian carbonate rocks, Arcturus Basin, Nevada and Utah: Brigham Young University Geology Studies, v. 17, pt. 2, p. 83–160.

Zoback, M.L., 1983, Structure and Cenozoic tectonism along the Wasatch fault zone, Utah: Geological Society of America Memoir 157, p. 3–27.

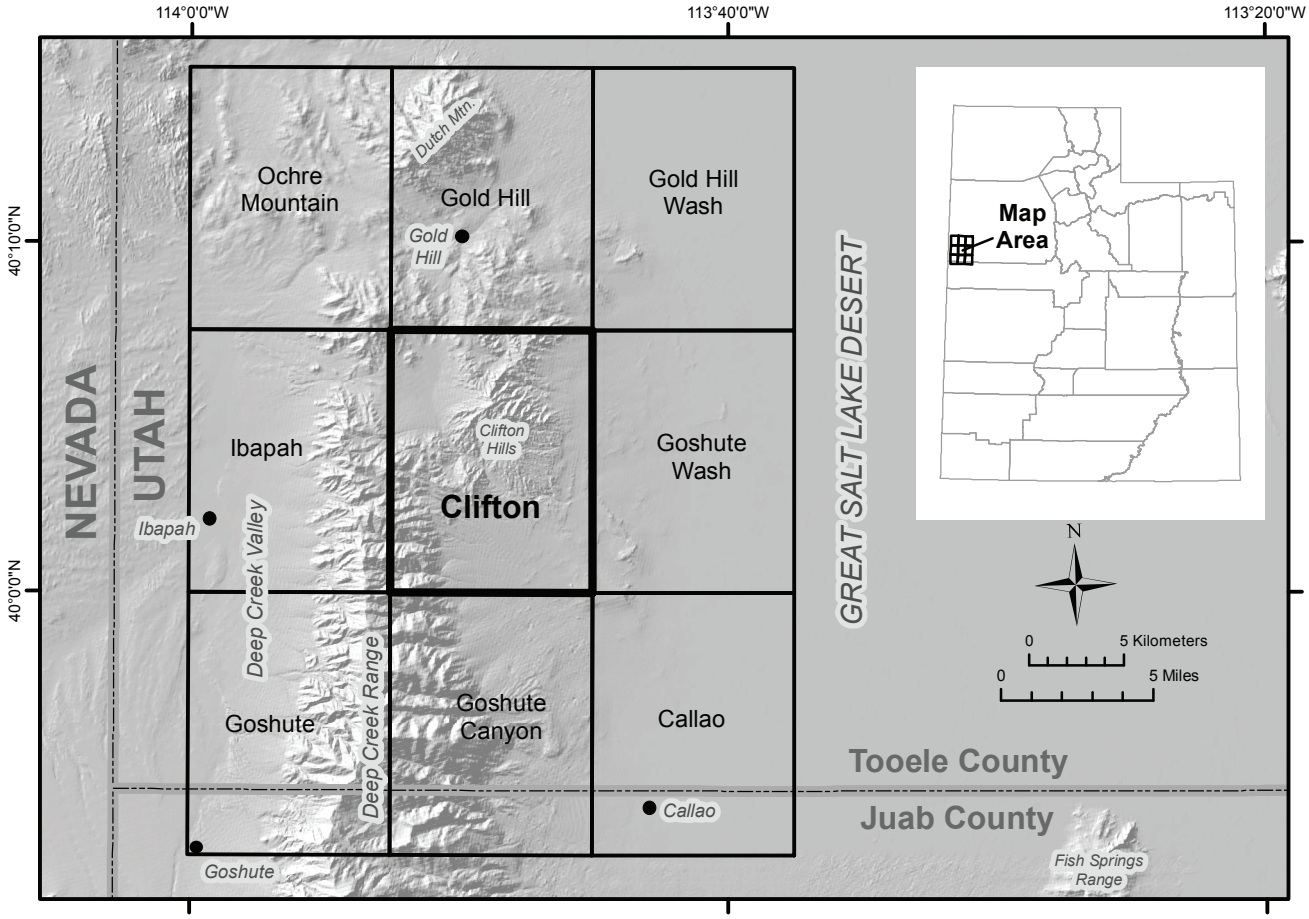

Figure 1. Location of and prominent geographic features near the Clifton quadrangle.

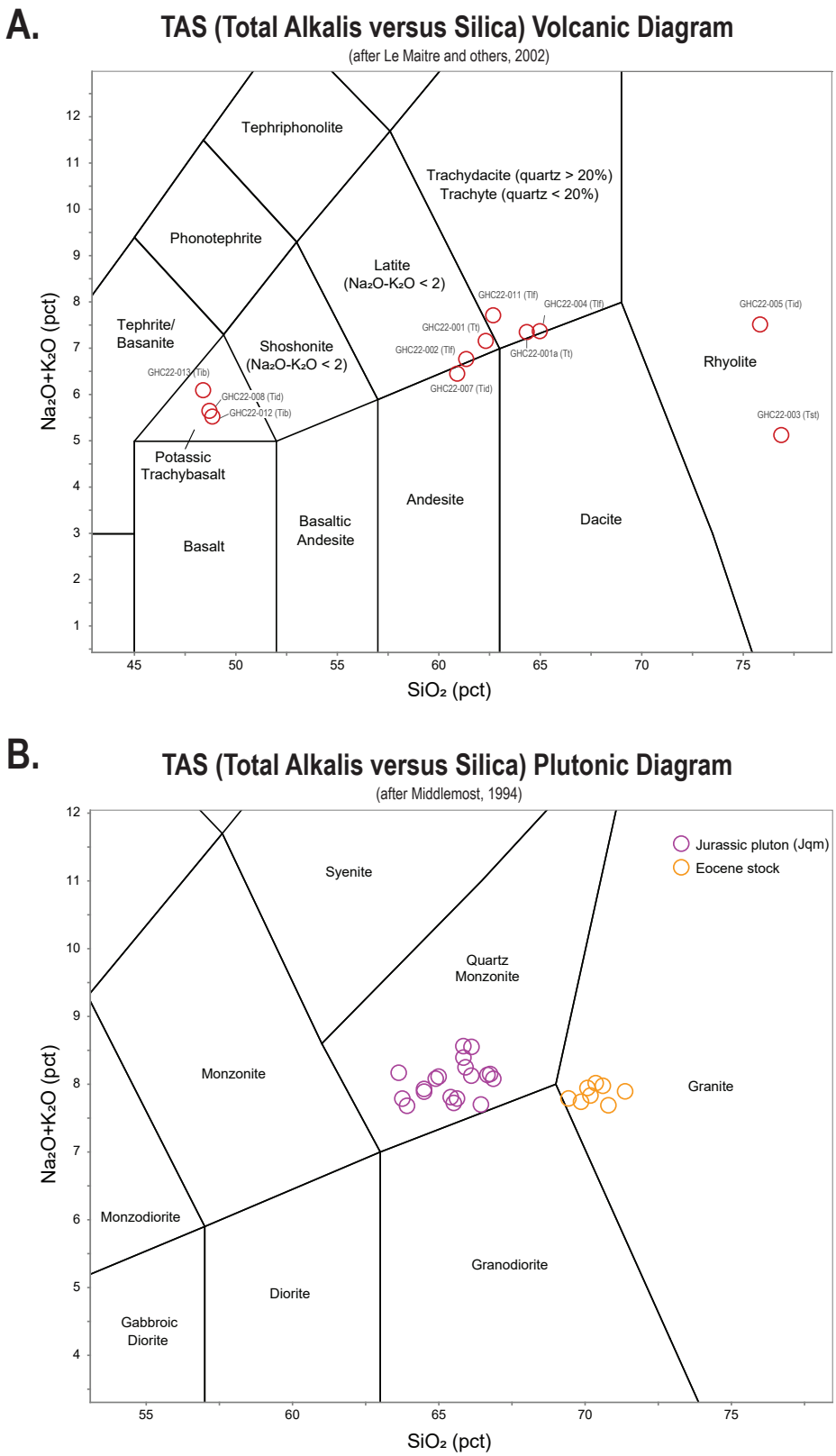

Figure 2. (A) *Total alkalis versus silica (TAS) volcanic diagram (Le Maitre and others, 2002) showing composition of samples collected in the Clifton quadrangle for this study. For rock classification purposes, the total of major element oxides (SiO_2, TiO_2, Al_2O_3, FeO MnO, MgO, CaO, Na_2O, K_2O, and P_2O_5) was normalized to 100% on the assumption of samples being water free and all iron occurring as FeO. All samples had Na2O-K2O < 2%; samples GHC22-001a and 004 had less than 20% quartz content and sample GHC22-011 had greater than 20% quartz content. Labels correlate with table 1 and plate 1.* ***(B)*** *TAS plutonic diagram (Middlemost, 1994) showing the composition of least altered samples of the Jurassic pluton in the Gold Hill and Clifton quadrangles and the Eocene stock in the Gold Hill quadrangle, collected as part of Mills (in progress).*

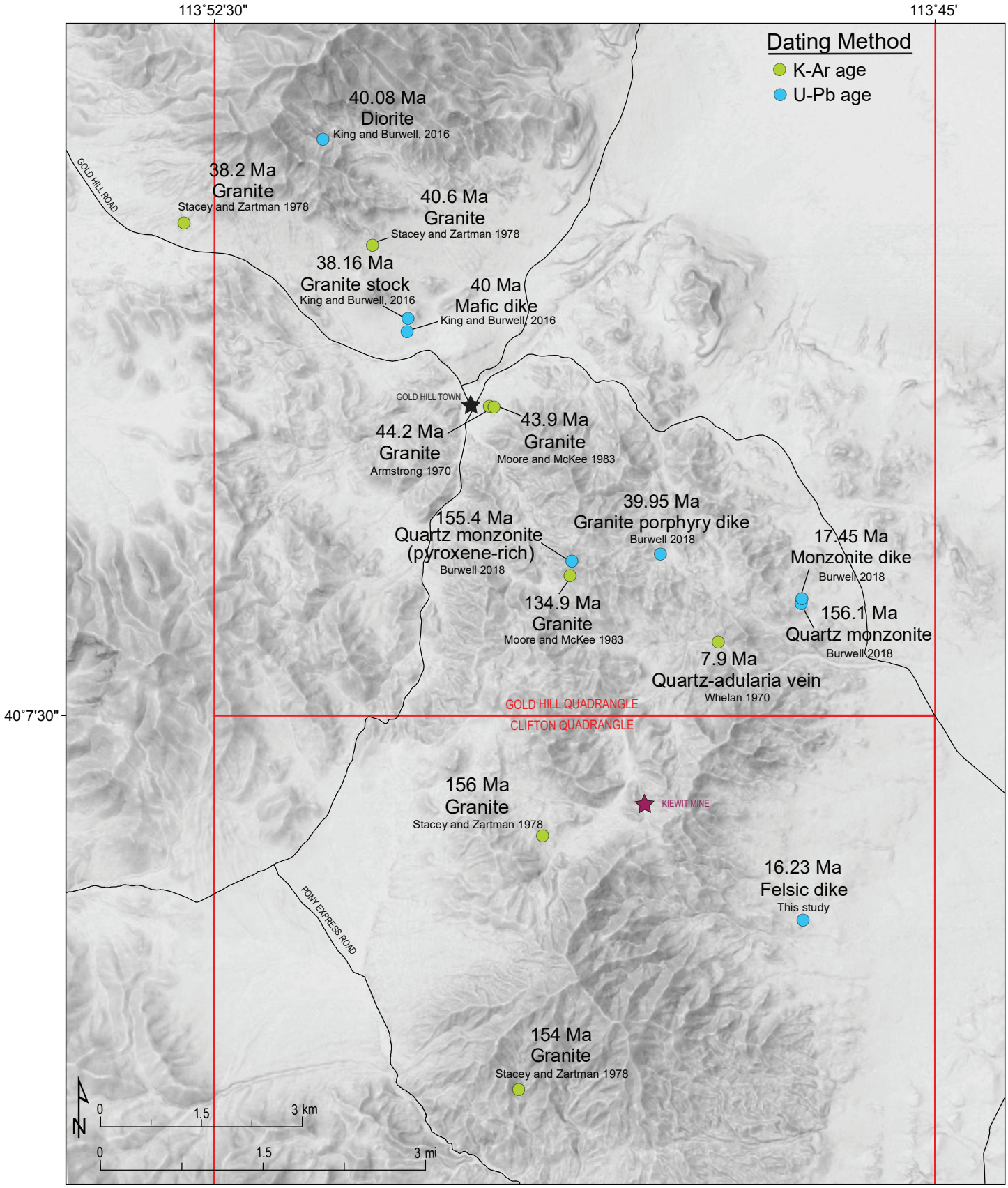

Figure 3. Map showing new and existing geochronology sample locations in the Gold Hill district, southern part of Gold Hill and northern part of Clifton quadrangles.

Table 1. *Major- and trace-element whole-rock geochemical data taken or referenced in this study.*

Map ID	UGS Sample ID	Map Unit	Date	Geologist	Easting	Northing	Datum	Source	TAS Rock Name	Field Sample Description	SiO2_ Norm_%	TiO2_ Norm_%	Al2O3_ Norm_%	Fe2O3_ Norm_%	MnO_ Norm_%	MgO_ Norm_%	CaO_ Norm_%	Na2O_ Norm_%	K2O_ Norm_%	P2O5_ Norm_%
1	GHC22-001	Tt	4/13/2022	SMills	257653	4445192	NAD83 Zone 12	This study	latite	Weathered dacitic to rhyolitic welded tuff	62.31	0.70	15.50	5.16	0.05	1.22	7.69	2.84	4.32	0.21
1a	GHC22-001a	Tt	9/26/2022	DClark	257653	4445192	NAD83 Zone 12	This study	trachyte	GHC22-001 resampled by DLC at a later date as to confirm geochemical composition	64.33	0.70	15.84	5.24	0.05	1.37	4.90	2.91	4.44	0.21
2	GHC22-002	Tlf	4/13/2022	SMills	257567	4445213	NAD83 Zone 12	This study	latite	Hard and blocky dark andesite, medium to fine grained, oxidation unavoidable along fractures	61.35	0.97	16.49	6.63	0.09	2.15	5.26	3.16	3.61	0.29
3	GHC22-003	Tst	4/13/2022	SMills	260871	4444977	NAD83 Zone 12	This study	rhyolite	Volcaniclastic sandstone, rhyolitic	76.87	0.29	12.54	3.03	0.03	0.52	1.52	0.88	4.24	0.07
4	GHC22-004	Tlf	4/13/2022	SMills	260845	4444838	NAD83 Zone 12	This study	trachyte	Fine-grained andesite volcanic rock, good outcrop blocky fracturing mildly porphyritic	64.97	0.84	16.89	5.61	0.05	0.70	3.30	4.49	2.87	0.26
5	GHC22-005	Tid	4/13/2022	SMills	263648	4442237	NAD83 Zone 12	This study	rhyolite	Felsic dike, green matrix with plagioclase phenocrysts, porphyritic texture	75.83	0.14	12.86	2.26	0.06	0.47	0.82	2.63	4.89	0.05
7	GHC22-007	Tid	4/13/2022	SMills	263599	4442349	NAD83 Zone 12	This study	andesite	Coarse grained mafic dike, least altered coarse grained mafic dike	60.90	1.38	14.89	7.28	0.12	3.14	5.40	2.91	3.53	0.45
8	GHC22-008	Tid	4/13/2022	SMills	263495	4442338	NAD83 Zone 12	This study	potassic trachybasalt	Fine-grained and coarse-grained mafic dike, fine grained may be chilled margin	48.70	2.70	16.50	11.47	0.16	5.25	8.80	3.17	2.48	0.78
11	GHC22-011	Tlf	4/13/2022	DClark	257720	4438121	NAD83 Zone 12	This study	trachydacite	Andesite porphyry	62.68	0.99	17.18	5.66	0.09	0.96	4.42	3.38	4.33	0.31
12	GHC22-012	Tib	4/13/2022	DClark	260197	4437903	NAD83 Zone 12	This study	potassic trachybasalt	Basalt dike	48.84	2.59	16.30	11.56	0.15	5.55	8.77	3.46	2.06	0.70
13	GHC22-013	Tib	4/13/2022	DClark	264597	4435624	NAD83 Zone 12	This study	potassic trachybasalt	Basalt	48.38	2.28	16.40	11.37	0.18	5.54	8.96	4.01	2.08	0.78
	KS2021-014		8/25/2021	KSmith	260008	4447671	NAD83 Zone 12	Mills (in progress)	quartz monzonite	No clear alteration or oxidation	63.92	0.76	15.20	5.12	0.08	2.73	4.04	3.46	4.22	0.47
	KS2021-017		8/25/2021	KSmith	260091	4446673	NAD83 Zone 12	Mills (in progress)	quartz monzonite		63.76	0.74	15.43	4.80	0.07	2.96	3.98	3.44	4.34	0.47
	KS2021-018		8/25/2021	KSmith	260430	4446642	NAD83 Zone 12	Mills (in progress)	quartz monzonite	No clear alteration or oxidation	64.90	0.67	15.29	4.70	0.07	2.22	3.58	3.68	4.40	0.49
	KS2021-021		8/25/2021	KSmith	260069	4446969	NAD83 Zone 12	Mills (in progress)	quartz monzonite	Limestone-quartz monzonite contact. Lots of alluvium but fairly certain this is in-situ. Limestone above quartz monzonite	63.64	0.67	16.74	4.47	0.07	1.92	3.85	4.26	3.91	0.47
	KS2021-024		8/25/2021	KSmith	260427	4446974	NAD83 Zone 12	Mills (in progress)	quartz monzonite	Finer grained than host rock. More resistant. Mafic composition?	65.92	0.67	15.04	4.86	0.07	2.21	2.51	3.53	4.72	0.47
	KS2021-026		8/25/2021	KSmith	259726	4447350	NAD83 Zone 12	Mills (in progress)	quartz monzonite		64.50	0.67	15.34	4.76	0.07	2.43	3.93	3.59	4.30	0.41
	KS2021-030		8/26/2021	KSmith	259400	4444519	NAD83 Zone 12	Mills (in progress)	quartz monzonite		66.66	0.60	14.88	4.21	0.06	2.23	2.87	3.58	4.55	0.36
	KS2021-038		8/26/2021	KSmith	258713	4444857	NAD83 Zone 12	Mills (in progress)	quartz monzonite	Mostly alluvium in this area. Uncertain alteration/intensity	65.00	0.63	14.49	4.09	0.06	2.60	4.64	3.35	4.76	0.38
	KS2021-055		9/8/2021	KSmith	259367	4444173	NAD83 Zone 12	Mills (in progress)	quartz monzonite		64.50	0.66	15.30	4.69	0.07	2.61	3.84	3.59	4.34	0.41
	KS2021-057		9/8/2021	KSmith	259735	4443519	NAD83 Zone 12	Mills (in progress)	quartz monzonite		65.63	0.60	15.22	4.38	0.07	2.39	3.55	3.55	4.24	0.37
	KS2021-061		9/8/2021	KSmith	258349	4445906	NAD83 Zone 12	Mills (in progress)	quartz monzonite		65.84	0.64	14.97	4.12	0.06	2.33	3.28	3.89	4.50	0.37
	KS2021-062		9/8/2021	KSmith	258338	4445903	NAD83 Zone 12	Mills (in progress)	quartz monzonite		65.84	0.64	15.13	4.04	0.06	2.44	2.92	3.86	4.70	0.38
	KS2021-066		9/8/2021	KSmith	259373	4447647	NAD83 Zone 12	Mills (in progress)	quartz monzonite		65.41	0.63	15.31	4.37	0.07	2.24	3.79	3.33	4.48	0.38
	SM21-022		9/21/2021	SMills	258689	4447329	NAD83 Zone 12	Mills (in progress)	quartz monzonite	Very coarse quartz monzonite weathering to grus with no obvious alteration	65.51	0.59	15.11	4.28	0.07	2.56	3.82	3.36	4.36	0.33
	TB2021-031		26/8/2021	TBoden	259034	4445244	NAD83 Zone 12	Mills (in progress)	quartz monzonite	Slighly greenish; eroded outcrop of quartz monzonite.	66.44	0.59	15.07	4.01	0.06	2.29	3.49	3.59	4.11	0.34
	TB2021-032		26/8/2021	TBoden	259395	4444866	NAD83 Zone 12	Mills (in progress)	quartz monzonite	Slighly greenish; eroded outcrop of quartz monzonite.	66.75	0.58	14.83	3.76	0.05	2.04	3.50	3.73	4.42	0.34
	TB2021-036		26/8/2021	TBoden	259034	4444862	NAD83 Zone 12	Mills (in progress)	quartz monzonite	Eroded outcrop of quartz monzonite.	66.86	0.56	15.17	3.63	0.05	1.91	3.42	3.78	4.30	0.32
	WH2021-008		9/8/2021	WHurlbut	260076	4444189	NAD83 Zone 12	Mills (in progress)	quartz monzonite	Pink/potassic or argillic alteration	66.11	0.59	15.07	4.10	0.07	2.21	3.38	3.62	4.50	0.35
	WH2021-028		9/8/2021	WHurlbut	259397	4445191	NAD83 Zone 12	Mills (in progress)	quartz monzonite	Minor alteration, subdued response to HCl	66.12	0.58	15.58	2.67	0.06	2.06	4.03	4.06	4.49	0.35
	BCJ2021-014		4/13/2021	BJordan	257404	4453466	NAD83 Zone 12	Mills (in progress)	granite	Outcrop extends down a steep hill slope, sample was taken from boulders at top for safety. uniform outcrop except for quartz veins.	69.85	0.46	14.61	3.16	0.06	1.38	2.61	3.08	4.66	0.12
	BCJ2021-017		4/13/2021	BJordan	258131	4453389	NAD83 Zone 12	Mills (in progress)	granite	Spheroidally weathered granite, uniform and unaltered	70.07	0.45	14.74	2.84	0.06	1.23	2.55	3.13	4.81	0.12
	BCJ2021-019		4/13/2021	BJordan	258559	4453015	NAD83 Zone 12	Mills (in progress)	granite	Isolated outcrop of granite, uniform throughout and spheroidally weathered with feox rind	69.42	0.51	14.26	3.40	0.06	1.55	2.87	3.03	4.75	0.14
	BCJ2021-021		4/13/2021	BJordan	257877	4453331	NAD83 Zone 12	Mills (in progress)	granite	Isolated outcrop of poorly competent granite with no major signs of alteration	70.35	0.42	14.62	2.74	0.05	1.21	2.46	3.07	4.94	0.12
	BCJ2021-023		4/13/2021	BJordan	257866	4452981	NAD83 Zone 12	Mills (in progress)	granite	Discontinuous spheroidally weathered granite outcrop, uniform throughout	70.78	0.40	14.35	2.74	0.06	1.30	2.57	3.11	4.58	0.11
	KS2021-001		8/23/2021	KSmith	257501	4452983	NAD83 Zone 12	Mills (in progress)	granite	Minor surficial feox	71.35	0.38	14.32	2.55	0.04	1.10	2.26	3.11	4.78	0.10
	KS2021-010		8/24/2021	KSmith	257155	4452981	NAD83 Zone 12	Mills (in progress)	granite		70.17	0.47	14.36	3.17	0.05	1.37	2.45	3.03	4.80	0.13
	KS2021-049		9/7/2021	KSmith	256815	4452977	NAD83 Zone 12	Mills (in progress)	granite		70.59	0.43	14.60	2.74	0.05	1.19	2.31	3.12	4.86	0.11

Table 1. *Continued*

Ag_ ppm	As_ ppm	B_ ppm	Ba_ ppm	Be_ ppm	Bi_ ppm	Cd_ ppm	Ce_ ppm	Co_ ppm	Cr_ ppm	Cs_ ppm	Cu_ ppm	Dy_ ppm	Er_ ppm	Eu_ ppm	Ga_ ppm	Gd_ ppm	Ge_ ppm	Hf_ ppm	Ho_ ppm	In_ ppm	La_ ppm	Li_ ppm	Lu_ ppm	Mn_ ppm	Mo_ ppm	Nb_ ppm	Nd_ ppm	Ni_ ppm	Pb_ ppm	Pr_ ppm	Rb_ ppm	Re_ ppm	Sb_ ppm	Sc_ ppm	Se_ ppm	Sm_ ppm	Sn_ ppm	Sr_ ppm	Ta_ ppm	Tb_ ppm	Te_ ppm	Th_ ppm	Tl_ ppm	Tm_ ppm	U_ ppm	V_ ppm	W_ ppm	Y_ ppm	Yb_ ppm	Zn_ ppm	Zr_ ppm
-0.5	-5		1045			0.5	122.5	16	97	3.8	30	6.37	3.17	1.68	19.9	7.5		9.97	1.24		68.3	20	0.45		2	25.5	51.5	27	25	14.05	175			12		9.86	2.7	343	1.8	1.11		30.5	-10	0.47	4.84	95	2	34.2	3.03	73	372
-0.5	7		1025			-0.5	120	16	109	4.05	34	5.82	2.97	1.63	21.7	7.12		9.43	1.13		65.2	20	0.4		2	26.5	49.2	30	29	13.85	176.5			12		9.23	2.7	353	1.8	0.99		30.5	-10	0.42	4.54	103	1.5	32	2.63	80	364
-0.5	-5		1350			-0.5	139	15	42	3.23	40	7.88	4.45	2.03	20.9	8.55		10.8	1.57		72.4	10	0.64		4	24.1	56.5	15	26	15.3	117.5			12		10.75	3.6	394	1.5	1.29		22.5	-10	0.64	4.54	145	1.9	43.6	4.15	88	415
-0.5	5		688			-0.5	97.1	2	19	2.25	4	2.66	1.43	0.9	15.1	3.32		4.67	0.5		54	30	0.24		1	14.6	33.5	6	18	10.15	146			4		5.37	1.9	126.5	1.2	0.48		19.9	-10	0.2	5.47	43	2.4	14.2	1.45	46	163
-0.5	-5		1495			-0.5	120	12	41	1.82	30	6.52	4.45	1.82	18.5	8.53		10.1	1.45		63.4	20	0.53		2	22.3	47	13	24	13.05	88.4			10		8.96	3.1	282	1.3	1.26		21.9	-10	0.51	4.67	187	1.9	34.7	3.38	73	370
-0.5	-5		179			-0.5	50.1	2	18	6.8	4	8	5.94	0.34	22.9	7.48		6.08	1.77		21.5	30	1.04		1	103.5	25	5	25	6.49	447			4		6.82	15.1	108.5	17.8	1.42		46.3	-10	0.93	15.55	15	12.4	54	7.23	54	134
-0.5	-5		531			-0.5	102	20	83	4.35	16	6	3.68	1.69	21	7.5		6.6	1.32		50.1	130	0.56		3	56.8	45.9	28	20	11.15	158			11		8.14	7.1	497	5.9	1.11		24.5	-10	0.69	11.05	124	3.1	36.7	3.93	85	244
-0.5	7		697			0.5	92.1	34	111	3.57	25	4.84	3.16	2.6	17.4	6.46		7.61	1.02		43.4	70	0.28		3	63.4	43.9	63	9	11.1	73.2			15		7.56	2.4	996	3.6	1.02		6.7	-10	0.41	1.7	190	1.7	27	2.32	92	284
-0.5	-5		1270			-0.5	138	11	12	4.37	14	6.69	3.73	2.4	20.4	8.3		10.45	1.42		74	20	0.46		2	25	57.5	6	23	15.8	158			10		8.64	3.1	361	1.4	1.05		23.9	-10	0.58	4.57	130	1.8	33.9	3.89	82	425
-0.5	5		792			0.5	97.1	40	159	0.88	29	5.32	2.56	2.26	19.2	8.38		7.14	1.01		47	10	0.31		2	47.1	45.8	94	7	12.05	49.1			18		7.05	1.3	780	2.6	0.94		5.74	-10	0.42	1.31	241	1.3	24.9	2.46	106	307
-0.5	-5		810			0.6	90.8	37	135	0.95	33	5.16	2.75	2.27	16.6	6.65		6.09	0.99		45.4	10	0.28		3	57.4	46.1	69	7	10.8	50.2			18		8.51	2.2	765	2.8	1.01		5.23	-10	0.37	1.4	222	2.2	25.8	2.58	97	250
-1	21	12	1440	-5	-0.1	-0.2	206	15.7	81	6.3	27	4.79	2.39	2.37	18.1	7.86	2	6	0.91	-0.2	112	109	0.29	573	-2	50.7	71.2	40	24	21	156	-0.02	5.5	10	-5	10.8	2	713	2.6	0.92	0.5	35.1	1	0.31	5.01	111	3	22.7	2	56	289
-1	17	16	1670	-5	-0.1	-0.2	227	18	84	4	60	4.96	2.55	2.43	19.5	8.14	2	6	0.96	-0.2	123	138	0.33	522	-2	58	75.4	49	29	22.1	156	-0.02	1.6	12	-5	11.8	3	723	3	0.96	-0.5	37.3	0.8	0.34	7.31	114	4	24.7	2.4	62	294
-1	6	15	1640	-5	0.1	-0.2	220	13.2	30	4.8	16	4.37	2.23	2.42	18.2	7.4	1	6	0.87	-0.2	121	58	0.29	591	-2	69.8	69.7	23	21	21.1	150	-0.02	0.5	8	-5	10.5	3	786	3.5	0.87	-0.5	31.7	0.8	0.32	7.21	93	3	22.4	2	50	280
-1	6	23	1720	-5	0.2	-0.2	224	12	26	5.9	43	4.22	2.09	2.54	19.7	6.91	2	6	0.8	-0.2	126	63	0.26	472	-2	57.8	69	23	23	20.8	144	-0.02	0.8	8	-5	10.2	3	939	2.7	0.82	-0.5	24.3	0.9	0.29	4.74	89	2	21.1	1.9	32	285
-1	12	24	1570	-5	0.5	-0.2	204	10.5	38	8.7	16	4.55	2.3	2.1	18.3	7.02	2	6	0.86	-0.2	111	83	0.3	531	-2	71.2	65.6	23	23	19.5	159	-0.02	1.1	8	-5	10	3	804	4.7	0.82	0.5	38.2	1.2	0.33	7.5	95	3	22.6	2.2	56	290
-1	8	32	1390	-5	0.4	-0.2	204	13.6	56	6.6	17	4.3	2.34	2.24	18.4	7.38	2	7	0.84	-0.2	108	80	0.3	547	2	51.6	66.7	36	32	19.3	169	-0.02	0.9	10	-5	10.3	2	718	3.3	0.86	-0.5	34	1	0.31	4.9	102	5	22.2	2.2	57	305
-1	5	13	1410	-5	0.3	-0.2	183	11.6	50	6.4	40	3.89	2.2	2.15	18	6.56	2	6	0.78	-0.2	102	76	0.33	484	-2	50.6	58.2	38	39	17.5	189	-0.02	0.9	9	-5	8.9	4	701	2.8	0.74	-0.5	36.5	1	0.29	6.83	84	28	20.2	2	52	254
-1	9	20	1490	-5	0.3	0.4	207	12.9	53	6	12	5.01	2.23	2.22	18.5	7.47	2	6	0.85	-0.2	116	58	0.3	418	2	53.3	70.9	23	46	21.2	199	-0.02	1	10	-5	10.9	3	684	3	0.86	-0.5	45.3	0.9	0.35	8.09	92	3	23.5	2.1	28	253
-1	6	11	1360	-5	0.1	-0.2	220	15.8	56	7.2	24	5.17	2.45	2.69	20.2	8.22	2	7	0.91	-0.2	120	43	0.29	557	-2	51.5	83	19	53	24	216	-0.02	1	9	-5	12.3	2	648	2.3	0.99	-0.5	40.7	1	0.39	6.27	100	4	24.8	2.2	59	308
-1	6	35	1230	-5	0.2	-0.2	207	14.2	60	7.2	24	4.93	2.42	2.52	18.7	7.53	2	6	0.83	-0.2	113	50	0.35	515	3	51.9	77.2	38	39	22.4	201	-0.02	1.4	8	-5	11.3	2	634	2.7	0.9	-0.5	42.2	0.9	0.33	8.18	85	11	24.5	2	38	274
-1	15	33	1410	-5	0.6	-0.2	234	10.4	52	5.3	15	4.7	2.17	2.26	20	6.81	3	5	0.84	-0.2	151	37	0.31	452	-2	53.5	71.7	19	45	22.4	192	-0.02	1.9	8	-5	10.6	4	719	2.7	0.89	-0.5	37	1.3	0.34	7.04	91	2	22	2.1	44	247
-1	14	35	1510	-5	0.5	-0.2	189	11	52	6.2	15	5.15	2.45	2.52	20	7.48	2	6	0.87	-0.2	98.4	40	0.35	484	-2	54.7	73.2	18	53	21.9	218	-0.02	1.9	9	-5	11	6	710	2.7	0.9	-0.5	39	1.5	0.35	7.54	95	2	24.8	2.2	41	292
-1	10	26	1460	-5	0.4	-0.2	181	11.8	64	5.6	14	4.52	2.17	2.07	19.4	7.06	2	6	0.78	-0.2	101	44	0.27	546	4	40.1	66	25	25	18.7	172	-0.02	1	12	-5	9.9	1	714	2.7	0.88	-0.5	36.2	0.9	0.3	4.44	90	3	22.1	2.1	67	243
-1	-5	-10	1450	-5	-0.1	-0.2	205	11.9	55	5.8	16	4.3	2.03	2.1	19.2	6.46	2	6	0.71	-0.2	115	50	0.26	573	4	36.9	64.4	30	30	18.4	177	-0.02	0.9	10	-5	9.4	2	688	2.6	0.84	-0.5	36.5	1.1	0.28	5.07	86	4	20.1	1.9	62	231
-1	19	166	1260	-5	1.4	-0.2	186	12.8	36	5.7	29	4.43	2.1	2.27	21.1	6.88	2	5	0.78	-0.2	102	58	0.39	450	-2	49.5	68.8	21	30	20.1	192	-0.02	2.1	9	-5	10.3	5	642	2.6	0.87	0.6	43	1	0.32	10.2	72	3	22	1.9	32	231
-1	15	72	1230	-5	1	-0.2	194	10.8	33	7.4	26	4.73	2.26	2.58	22.6	7.42	2	6	0.82	0.2	104	26	0.33	408	2	59.3	70.9	18	55	21.1	199	-0.02	1.5	8	-5	11.4	13	612	3	0.89	-0.5	47.8	1	0.36	11.4	71	3	25.6	2.1	47	295
-1	10	90	1230	-5	0.3	-0.2	176	9.6	37	5.1	13	4.25	2.1	2.22	20.5	6.48	2	5	0.76	-0.2	94.1	31	0.31	352	-2	45.8	64.3	22	39	19.2	174	-0.02	0.9	8	-5	9.7	6	654	2.1	0.81	-0.5	34.9	0.8	0.33	5.97	65	3	21.7	2	18	241
-1	6	-10	1340	-5	0.2	-0.2	181	11.7	64	6	21	4.3	2.1	1.94	21.5	6.25	2	6	0.76	-0.2	102	50	0.27	603	4	48.1	62.1	36	43	17.5	184	-0.02	1.2	13	-5	9.2	-1	695	3.8	0.78	-0.5	42.6	1	0.29	8.29	75	4	21.1	2	82	237
-1	16	81	1590	-5	0.2	-0.2	148	6.8	60	5.9	6	3.92	1.98	1.97	20	5.67	2	6	0.66	-0.2	82.4	32	0.25	493	4	42.9	50.7	24	46	13.8	150	-0.02	2.1	13	-5	8.1	5	669	2.9	0.69	-0.5	31.9	0.9	0.27	6.77	73	3	19.7	1.8	66	262
-1	-5	-10	801	-5	-0.1	-0.2	137	7.6	97	3.6	9	5.46	3.05	1.09	24.3	6.35	1	7	1.04	-0.2	75	37	0.41	376	-2	26.3	45.6	45	34	13.4	237	-0.02	-0.1	6	-5	7.9	6	191	1.9	0.87	-0.5	42.9	1.3	0.44	4.29	55	-1	30.8	3.2	53	289
-1	-5	-10	1020	-5	-0.1	-0.2	119	6.4	39	3.3	8	5.29	3.01	1.12	22.1	6.3	1	6	1.01	-0.2	64.5	50	0.43	355	-2	25.2	41.5	27	33	12.1	215	-0.02	-0.1	7	-5	7	6	247	1.8	0.88	-0.5	43.3	1.2	0.46	4.1	49	-1	29	3.2	27	246
-1	-5	-10	798	-5	-0.1	-0.2	146	9.6	32	5.7	24	7.56	4.47	1.43	26.1	8.4	2	9	1.46	-0.2	75.3	55	0.61	394	-2	35.9	53	49	39	14.9	283	-0.02	0.2	7	-5	9.3	8	181	2.8	1.19	-0.5	60.7	1.3	0.69	9.15	59	-1	43.5	4.6	51	348
-1	-5	-10	872	-5	-0.1	-0.2	131	6	85	3.3	9	5.03	2.88	1.07	21.9	6.01	1	7	0.97	-0.2	72.9	34	0.39	346	-2	22.4	43.2	36	32	12.6	211	-0.02	-0.1	-5	-5	7.1	5	191	1.6	0.82	-0.5	42.1	1.1	0.42	5.32	48	-1	27.7	2.9	47	290
-1	-5	-10	736	7	0.1	-0.2	126	5.7	45	4.6	8	5.2	3.12	0.95	22.8	5.89	1	7	1.05	-0.2	68.1	43	0.48	348	-2	27.8	41.5	16	34	11.9	233	-0.02	-0.1	5	-5	7	6	181	2.2	0.87	-0.5	42.6	1.2	0.47	5.47	46	1	30.2	3.2	51	255
-1	-5	-10	829	-5	-0.1	-0.2	95.7	5.5	25	4.1	15	4.43	2.73	1.03	19.9	4.96	2	6	0.88	-0.2	50.2	114	0.4	325	-2	26.8	31.6	10	42	9.75	234	-0.02	0.7	6	-5	5.6	4	221	1.9	0.73	-0.5	35.6	1.3	0.4	4.59	44	3	25.4	2.7	41	264
-1	-5	-10	927	-5	-0.1	-0.2	136	6.9	36	4.5	25	5.97	3.69	1.05	20.8	7.25	2	7	1.24	-0.2	71.6	100	0.54	426	-2	31.2	45.2	10	34	13.4	223	-0.02	0.6	7	-5	7.9	6	220	2.3	0.99	-0.5	44.2	1.3	0.51	4.65	56	1	34.7	3.5	54	297
-1	-5	16	948	5	0.4	-0.2	132	7	22	5.2	55	5.63	3.11	1.25	22.1	6.63	2	5	1.12	-0.2	71.1	48	0.5	334	-2	26.5	47.1	-5	38	14.4	264	-0.02	0.7	6	-5	8.3	5	234	1.6	0.95	-0.5	43.5	1.4	0.5	7.09	43	10	33.6	3.2	31	231

Notes:
Volcanic rock samples map ID and map unit correspond to plate 1 (this study).
Plutonic rock samples from Clifton and Gold Hill quadrangles (Mills, in progress).
Rock names for this study are from total alkalis-silica (TAS) diagrams of Le Maitre and others (2002) and Middlemost (1994).
Analyses for this study performed by ALS Global (volcanic rocks) and USGS (plutonic rocks).
Major oxides reported in weight percent (%); negative values are below detection limit.
Minor and trace elements reported in parts per million (ppm); negative values are below detection limit.
Major oxides have been normalized on a 100% water-free basis.
Blank values indicate an element was not measured for a given sample.

Table 2. *Summary of new and existing geochronology in the Gold Hill district.*

Map ID	Sample ID	Easting	Northing	Datum	Sample Type	Age (Ma)	Error (Ma)	Revised Age (Ma)	Revised Error (Ma)	Mineral	Method	Source
10	GHC22-010	263556	4442284	NAD83 Zone 12	Felsic dike (unit Tid)	16.23	0.26			Zircon	U-Pb	This study
	8	259122	4450086	NAD83 Zone 12	Granite	42.5	0.8	44.2	0.8	Biotite-hornblende	K-Ar	Armstrong, 1970
	GXJ256085	263675	4446959	NAD83 Zone 12	Monzonite dike	17.14	0.4			Zircon	U-Pb	Burwell, 2018
	GXJ256081	261612	4447769	NAD83 Zone 12	Granite porphyry dike	39.95	0.47			Zircon	U-Pb	Burwell, 2018
	GXJ256076	260301	4447703	NAD83 Zone 12	Quartz monzonite (pyroxene-rich)	155.4	1.8			Zircon	U-Pb	Burwell, 2018
	GXJ256084	263686	4447042	NAD83 Zone 12	Quartz monzonite	156.1	1.8			Zircon	U-Pb	Burwell, 2018
	GH-002	257986	4451361	NAD83 Zone 12	Granite stock	38.16	0.45			Zircon	U-Pb	King and Burwell, 2016
	GH-001	257972	4451168	NAD83 Zone 12	Mafic dike	40	0.56			Zircon	U-Pb	King and Burwell, 2016
	GH-006	256815	4454054	NAD83 Zone 12	Diorite	40.08	0.56			Zircon	U-Pb	King and Burwell, 2016
	74-KA-15	247401	4453710	NAD83 Zone 12	Latite	39.2	0.6			Biotite	K-Ar	Moore and Mckee, 1983
	74-KA-16	259359	4450078	NAD83 Zone 12	Granite	43.9	0.8			Biotite	K-Ar	Moore and Mckee, 1983
	74-KA-9	260227	4447581	NAD83 Zone 12	Granite	134.9	4			Hornblende	K-Ar	Moore and Mckee, 1983
	70-2	254752	4452634	NAD83 Zone 12	Granite	37.4	1.3	38.23	1.3	Biotite	K-Ar	Stacey and Zartman, 1978
	6	257448	4452547	NAD83 Zone 12	Granite	39.7	1.4	40.62	1.4	Biotite	K-Ar	Stacey and Zartman, 1978
15A	15A	259035	4439902	NAD83 Zone 12	Granite	151	5	154.32	5	Biotite	K-Ar	Stacey and Zartman, 1978
18	18	259727	4443769	NAD83 Zone 12	Granite	153	5	156.46	5	Biotite	K-Ar	Stacey and Zartman, 1978
	unknown	262306	4446533	NAD83 Zone 12	Quartz-adularia vein	8	0.8	7.85	0.8	Adularia	K-Ar	Whelan, 1970
	Alln006	257986	4451354	NAD83 Zone 12	Granite stock	37.74	3.86			Allanite	UPb	Burwell, 2018
	Alln0042	256815	4454047	NAD83 Zone 12	Granite stock	42.55	4.35			Allanite	UPb	Burwell, 2018
	GHTIT-002	260336	4447682	NAD83 Zone 12	Quartz monzonite	158.57	15.8			Titanite	UPb	Burwell, 2018
	GHTIT-003	260336	4447682	NAD83 Zone 12	Quartz monzonite	156.2	9.38			Titanite	UPb	Burwell, 2018
	GHTIT-004	263048	4447485	NAD83 Zone 12	Quartz monzonite	160.36	9.12			Titanite	UPb	Burwell, 2018
	GH-070	260247	4447768	NAD83 Zone 12	Quartz monzonite	157.53	11.17			Titanite	UPb	Burwell, 2018
	GXJ25006	257986	4451354	NAD83 Zone 12	Granite stock	49.58	2.73			Titanite	UPb	Burwell, 2018

Notes:
Map ID corresponds to plate 1.
Revised ages and errors reported in the USGS geochronology database (2023). Revised using new decay constants (see for example, Dalrymple, 1992).
Italicized entries are not included on the map in figure 3 because they represent method testing rather than robust ages.
Locations for older samples are approximate.